University of Nevada, Reno

Adaptation and the Perception of Radiological Images

A dissertation submitted in partial fulfillment of the
Requirements for the degree of Doctor of Philosophy in
Psychology

By

Elysse J. Kompaniez-Dunigan

Dr. Michael A. Webster/Dissertation Advisor

May, 2014

THE GRADUATE SCHOOL

University of Nevada, Reno
Statewide · Worldwide

We recommend that the dissertation
prepared under our supervision by

ELYSSE J. KOMPANIEZ-DUNIGAN

entitled

Adaptation And The Perception Of Radiological Images

be accepted in partial fulfillment of the
requirements for the degree of

DOCTOR OF PHILOSOPHY

Dr. Michael A. Webster, Advisor

Dr. Michael Crognale, Committee Member

Dr. Anne Leonard, Committee Member

Dr. Lars Strother, Committee Member

Dr. Van der Linden, Graduate School Representative

Marsha H. Read, Ph. D., Dean, Graduate School

May, 2014

Abstract

Radiologists must classify and interpret medical images on the basis of visual inspection. We examined how an observer's visual sensitivity and perception might change as they view and thus adapt to the characteristic properties of radiological scans. Measurements were focused on the effects of adaptation to images of normal mammograms, and were tested primarily in observers who were not trained radiologists. Mammograms have steeper power spectra (slopes of ~-3) than natural images (~-2) and thus are physically blurry. Adapting to them produced shifts in the perceived spectrum of filtered noise consistent with adaptation to blur, even though this adaptation does not lead to measurable changes in the contrast sensitivity function. Strong aftereffects in the appearance of the images were also found when observers judged the perceived texture of the images. For example, tissue density in mammograms is routinely classified and ranges from "dense" to "fatty." Adaptation to dense images caused an intermediate image to appear more fatty and vice versa. Our results thus suggest that observers can selectively adapt to the properties of radiological images, and this could potentially be an important factor in the perception and learning of radiological images. In a further study we explored whether adaptation could enhance visual inspection of radiological images, specifically to aid observers in identifying abnormalities by adapting out or discounting the expected visual characteristics of the background. Observers searched for simulated lesions (Gaussian targets) added at random locations in the images. Prior adaptation to

the images allowed the targets to be located more quickly, and this performance gain was selective for the tissue type and thus the visual texture defining the background. These improvements in visual search provide a novel demonstration of the advantages of spatial pattern adaptation within contexts that closely mimic routine visual tasks and settings. Finally, we explored the neural correlates of these adaptation aftereffects by measuring ERP's while observers adapted to the different textural properties of the mammogram images (dense or fatty). There was no significant difference of adapt condition in the component waveforms when tasked with categorizing the scans based upon their density classifications. In contrast, there was a significant effect of adaptation when observers were signaling target presence or absence. This significant difference was characterized by an enhancement of the neural response at early timepoints in occipital areas. Additionally, following adaptation we observed a divergence in the target present and absent waveforms at approximately 370 ms post-stimulus onset in frontal recording sites. These results suggest that target detection involves a form of the P300 component. Taken together these studies represent the first comprehensive analysis of the influence of adaption on the critically important visual judgments involved in interpreting and inspecting medical images.

Acknowledgements

I would like to express my sincere gratitude to my advisor Dr. Michael Webster. Throughout my graduate career he has provided me with guidance, enthusiastic encouragement and the independence to develop and pursue my own research questions. His support and thoughtful advice has been invaluable to my graduate success and I feel fortunate to have had such an inspirational mentor.

I would like to offer special thanks to my dissertation committee members, Dr. Lars Strother, Dr. Michael Crognale, Dr. Anne Leonard and Dr. Alexander Van der Linden for their insightful and valuable comments and suggestions.

I would also like to extend my thanks to past and present members in the Visual Perception Laboratory who have provided me with continual support and contributions to my research. I am particularly grateful for the friendships I have developed while attaining my doctoral degree. Especially Dan, Kevin and Dwight for continually putting up with my endless stress and having an incredible ability to put me at ease.

I want to especially thank my parents and sister who have inspired me to pursue my goals at all costs, encouraged me to ask thought provoking questions and have taught me the value of giving back to others. Without them I would not be the individual I am today.

Finally, I would like to thank my husband Jim Dunigan who has provided day to day love and encouragement. He has motivated me to see things from a

different perspective and to approach each day with optimism. I feel truly lucky to have such an inspiring, supportive and creative husband.

Table of Contents

List of Figures

I. Introduction

A wealth of evidence suggests that visual perception is adapted over both long and short timescales to be optimized for coding information about the natural visual environment. At long durations, the natural world has characteristic properties, and these properties are thought to have shaped the evolution of visual mechanisms so that they can efficiently represent the content of images in order to support important tasks such as finding, recognizing, and interpreting the objects and scenes before us (Simoncelli & Olshausen, 2001). At short timescales, the statistics of scenes vary from one environment to the next, and processes of adaptation are thought to adjust to these variations to match visual coding for the current context (M. A. Webster, 2011a). In this work, I have explored the consequences of these short-term adaptation processes when observers must make important visual judgments within "unnatural" environments. Increasingly, humans are exposed to novel visual worlds created by our technology (e.g. video games) or accessed through technology (e.g. remote sensing). How does the visual system adapt to these new worlds, and what are the implications of this adaptation for how and how well we can see? In this work, I explore these questions by exploring the effects of adaptation on perception within a specific environment – in an observer inspecting medical images.

Radiologists spend hours at a time examining medical images and making crucial diagnostic decisions about them. Despite advances in assistive technologies such as computer-aided detection algorithms, the evaluation and

interpretation of medical images still relies ultimately on visual inspection by humans, and thus remains fundamentally constrained by the perceptual and cognitive capacities of the observer (E. A. Krupinski, 2011). For example, the evaluation of medical images depends upon subjective visual judgments and approximately 30-40% of false negative errors in clinical radiology are thought to be perceptual (Gale, 19884; Kundel, 2004; Manning, Gale, & Krupinski, 2005). Many studies have investigated the visual processes that impact visual judgments about medical images including factors influencing detection and discrimination of patterns (Burgess, Jacobson, & Judy, 2001; Burgess, Li, & Abbey, 1997), the properties of visual search and salience (Drew, Evans, Vo, Jacobson, & Wolfe, 2013; M. P. Eckstein, 2011; Evans, Birdwell, & Wolfe, 2013), and the role of perceptual learning and expertise (Snowden, Davies, & Roling, 2000). Common to each of these studies has been the attempt to understand how standard visual processes and constraints are manifest in the context of the specific stimulus statistics characterizing medical images (Bochud, Abbey, & Eckstein, 1999; M.P. Eckstein, Abbey, & Bochud, 2000).

In these studies, I explore the role of a further well-known perceptual process that is intimately linked to the visual structure defining the image – visual adaptation. The sensitivity and response properties of the visual system are constantly adjusted through adaptation to match visual coding to the attributes of the stimuli we are currently viewing (C. W. Clifford et al., 2007; Kohn, 2007; M. A. Webster, 2011a). Here I ask whether these adjustments occur for attributes of medical images in ways that could influence how such images are perceived and

classified. Specifically, I have explored the effects of adaptation on the perception of mammogram images. The following provides a general overview of this work.

Adaptation and the perception of medical images

Visual coding is constantly modulated by adaptation processes that adjust sensitivity according to the stimuli to which observers are currently exposed (C. W. Clifford et al., 2007; Kohn, 2007; M. A. Webster, 2011b). These changes can profoundly affect the appearance of images, illustrated by many classical perceptual aftereffects (Thompson & Burr, 2009; M. A. Webster, 2011b). For example, the perceived color, shape or direction of motion can be strongly biased by exposure to a different stimulus (e.g. a gray field appears reddish after adapting to a green field, and a circular ellipse appears stretched vertically after adapting to a horizontally elongated ellipse). Moreover, aftereffects are invoked by patterns we typically encounter in natural viewing conditions (Bex, Solomon, & Dakin, 2009; M. A. Webster & Miyahara, 1997) and extend to higher-level and ecologically important visual judgments, resulting for example in changes in the perception of a face (M. A. Webster & MacLeod, 2011) or the perceived spatial layout of a scene (Greene & Oliva, 2010) . Importantly, natural viewing conditions can affect the observer's state of adaptation, and changes in surroundings or viewing conditions thus result in changes in these states. Furthermore, the natural environment has characteristic statistical properties for which the visual system may be routinely adapted (Field, 1987; Field & Brady, 1997; Tolhurst,

Tadmor, & Chao, 1992) This raises the question of how well visual coding can adjust to and operate within environments with unnatural statistics.

Medical images provide an ideal context for probing the processes and consequences of visual adaptation because these images have well defined properties that differ from the statistics of natural images. For instance the power spectra (the amount of energy present in the frequency components) of medical images is typically steeper than natural spectra (Burgess et al., 2001). This reduction in amplitude at higher spatial frequencies results in the image appearing blurrier in appearance relative to images that have natural spectra. Furthermore, previous studies have demonstrated that images with steeper power spectra than that of natural stimuli induce rapid and strong blur aftereffects. Thus, simply viewing medical images could induce adaptation effects that could influence their appearance. Again, radiologists can spend prolonged periods inspecting images to make diagnostic decisions, and thus this exposure is likely to lead to pronounced adaptation.

Density Classification

Radiologists not only inspect mammograms for lesions and tumors, they also classify the images based upon their textural properties. The BI-RADS Density classification system is used to rate the breast tissue on a scale from fatty to dense ((ACR), 1998). A rating of fatty implies the tissue is composed entirely of fat, and is characterized by a striated appearance (Figure 1, bottom row). A rating of dense instead signifies the presence of fibroglandular tissue,

Dense - (BIRADS 4)

Fatty - (BIRADS 1)
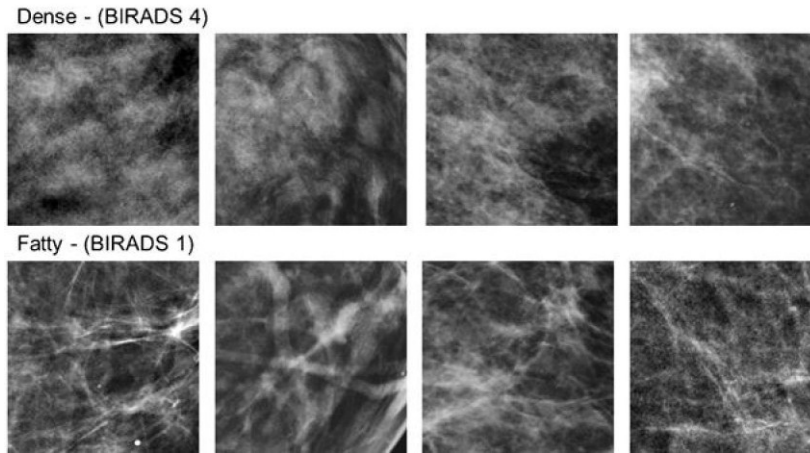
Figure 1. Examples of image sections from mammograms classified as dense or fatty.

and corresponds to an image that appears cloudier in nature (Figure 1, top row). Dense tissue significantly lowers the sensitivity of a mammogram (Hersh & Marla, 2004) often due to obscuring lesion detection (Boyd, 2011). Moreover, these classifications are important because they are related to the potential prevalence of cancer. For example tissue density has been correlated with four to six times greater incidence of breast cancer (Boyd et al., 2007) and women who were administered Tamoxifen (a prescription drug that changes breast density) and showed a marked reduction in density revealed a 63% decrease in the risk of breast cancer (Boyd, 2011). Complications can arise when visually inspecting the image and rendering a decision based upon inspection, suggesting perception plays a significant role when making diagnostic decisions (E. A. Krupinski, 2011). Thus whether an image appears dense or fatty has important implications for patient health and for subsequent diagnostic tests.

Amplitude Spectra of Medical Images and Blur Perception

As stated earlier, mammogram images have different image statistics than that of natural scenes, specifically natural images generally have a shallower

(Figure 2, dashed line) power spectra than that of medical images (Figure 2, solid line) (Burgess et al., 2001).This reduction in amplitude at high spatial frequencies is similar to image blur (Field & Brady, 1997), which is known to induce rapid and strong adaptation (Elliott, Georgeson, & Webster, 2011; Vera-Diaz, Woods, & Peli, 2010; M. A. Webster, Georgeson, & Webster, 2002). This is demonstrated by the finding that viewing a blurred image for a short duration causes a focused image to appear over-sharpened or vice versa (Webster, Georgeson et al. 2002; Vera-Diaz, Woods et al. 2010; Elliott, Georgeson et al. 2011). Moreover, prolonged exposure to blurred or sharpened images resulted in the images appearing better focused over time suggesting adaptation functions to maintain the perception of focus despite changes in the environment or observer (Elliott et al., 2011).

Adaptation not only affects the perceived blur of images, but can also alter threshold sensitivity
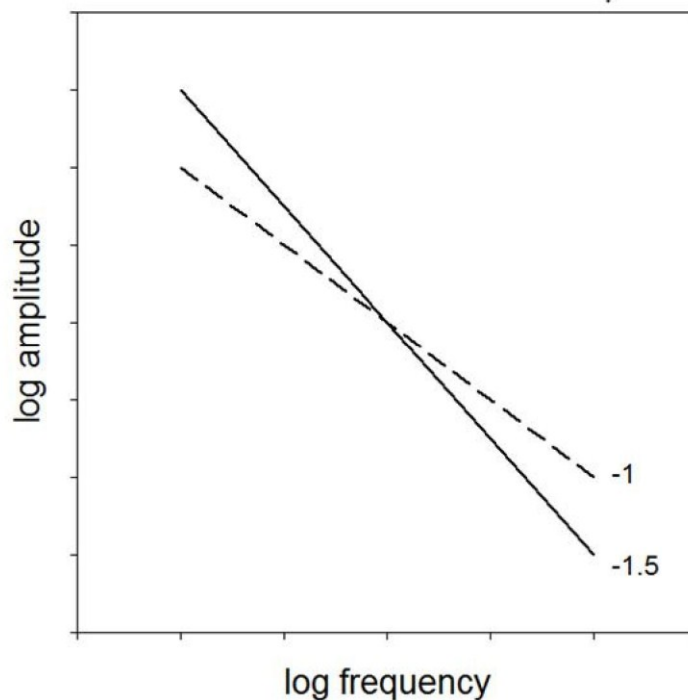
Figure 2. Amplitude spectra of natural images (dashed line) vs. medical images (solid line). Medical images have a reduction in amplitude at high spatial frequencies causing them to appear "blurrier" than natural images.

to spatial patterns. These thresholds are typically measured by the contrast

sensitivity function (CSF), which plots the sensitivity to contrast as a function of

spatial frequency. The CSF is a standard metric for characterizing spatial

vision(De Valois & De Valois, 1990) and for predicting visual performance in

medical image perception (Burgess et al., 2001). Adaptation to the characteristic

properties of natural images (more energy at low-to-medium spatial frequencies)

results in a sensitivity loss to low-to-medium spatial frequencies, altering the

shape of the contrast sensitivity function (CSF) (Bex et al., 2009; M. A. Webster

& Miyahara, 1997). Adaptation also reduces the perceived suprathreshold

contrasts at low frequencies compared to higher frequencies (M. A. Webster &

Miyahara, 1997). It remains unclear how these contrast changes are related to

changes in the perception of image focus, or how selective the adaptation is for

the specific amplitude spectrum of the adapting images. For example, Webster

and Miyahara (1997) found little difference in the shape of the CSF following

adaptation to images with natural vs. more blurred spectra (M. A. Webster &

Miyahara, 1997), even though these images differ markedly in the blur

aftereffects they induce (M. A. Webster et al., 2002).

Adaptation and visual search in mammograms

Ultimately radiologists are faced with the challenging task of searching for

lesions and tumors within the breast tissue, and locating these abnormalities has

obvious health consequences. There has been an extensive amount of research

investigating the manner in which radiologists search medical images and in

efforts to improve detection accuracy and efficiency. Many studies have shown that radiologists are able to rapidly extract a great deal of information from these images (Drew et al., 2013; E.A . Krupinski, 1996; Kundel & Follette, 1972; Kundel & Nodine, 1975; Kundel, Nodine, Krupinski, & Mello-Thomas, 2008; Mugglestone, Gale, Cowley, & Wilson, 1995). The initial inspection of the images gives rise to a global impression which then acts as a filter to direct attention to areas of further interest (Kundel, Nodine, Thickman, & Toto, 1987; Swensson, 1980). Importantly, this initial stage enables radiologists to compare the image under inspection to prior knowledge of normal structures within the image. When given a short duration (200 ms) to inspect chest radiographs, radiologists performed surprisingly well, with approximately a 70% correct response rate (Kundel & Nodine, 1975). This brief presentation allows for only one initial eye fixation, revealing that radiologists rapidly extract a great deal of information from the image in parallel, and are able to make diagnostic decisions based upon this initial representation. This was also observed when radiologists were tasked with inspecting mammogram images (Mugglestone et al., 1995) with approximately 67% of the locations containing cancers being located within 1 sec (Kundel et al., 2008). The ability to be able to make a diagnostic decision based upon a rapid global impression is likely due to the expert radiologist comparing the image under inspection to that of an internal representation of what is expected (normal) in the image and what is abnormal. This is supported by changes in search patterns through experience and training (Kundel & Follette, 1972) and further evidenced by the fact that experienced readers detect targets more quickly (E.A .

Krupinski, 1996) and more accurately than those of less experienced readers (Donovan & Litchfield, 2013; Snowden et al., 2000). Furthermore, novices improved through training, indicating detection of targets can be enhanced through sensory learning processes (Snowden et al., 2000). Despite this if target prevalence is low(Gur et al., 2004), which is the case in routine mammography screenings, observers error rates increase (Horowitz, Kenner, & Wolfe, 2005; Wolfe et al., 2007). This is due to the fact that rare targets are often missed because participants do not expect them in a large portion of the images. Thus satisfaction of search, the amount of time given to inspecting the image prior to moving to the next scan, is reached more quickly than tasks with increased prevalence of targets (Horowitz et al., 2005; Wolfe et al., 2007). Thus, understanding ways in which to optimize visual inspection of radiological scans is a continuing avenue of research.

Although a great deal of research has been devoted to investigating the visual factors influencing search within medical images, little to none has explored the role of adaptation and visual search within mammograms. Visual adaptation influences not only the appearance of images, but visual performance – how accurately or quickly observers can make judgments or detect information within the images. Adaptation has been shown to improve discrimination tasks across a wide range of stimuli including, but not limited to, orientation, speed judgments, tilt and contrast (Abbonizio, Langley, & Clifford, 2002; C. W. G. Clifford, Wyatt, Arnold, Smith, & Wenderoth, 2001; Kristjánsson, 2011). Many of these studies investigated enhancements in threshold discrimination tasks, but

have not looked at improvements in a suprathreshold task such as visual search. McDermott and colleagues (McDermott, Malkoc, Mulligan, & Webster, 2010) investigated if adaptation could increase the salience of chromatic targets relative to a chromatic background. They found that observers were better able to detect novel colored targets following adaptation to a background color distribution, suggesting adaptation affects the salience of the target relative to the background. Additionally, adaptation improved accuracy and decreased reaction times when searching for Gabor targets within a set of distracters (Wissig, Patterson, & Kohn, 2013). These studies reveal adaptation may function to highlight salient targets or novel structure within an environment by decreasing the sensitivity to the prevailing background structure.

Neural correlates of adaptation and medical image perception

A whole field of research has explored the neural mechanisms mediating perceptual judgments, including the temporal dynamics of scene and object recognition. Understanding these dynamics has allowed researchers to dissect when and where in the visual processing stream recognition is occurring. In particular, utilizing electroencephalogram (EEG) readings of the cortex, investigators have been able to tease apart how computations are performed in the visual processing stream. A large body of evidence suggests that recognition of natural scenes is a fast, feed-forward process (Anokhin et al., 2006; Antal, Kéri, Kovács, Janka, & Benedek, 2000; Antal et al., 2001; Thorpe, Fize, & Marlot, 1996). These studies investigated individuals' ability to recognize an animal in a

natural scene context and correctly respond whether or not an animal (target) was present.

Thorpe and colleagues (Thorpe et al., 1996) found that participants were remarkably good at this task, responding correctly 94% of the time, despite images being displayed for only 20 ms. Utilizing event-related potentials (ERPs) and a go/no-go task; where observers were to respond just to target presence (animal in the image), they observed a divergence in the average waveforms at approximately 150 ms. This divergence was characterized by a greater negative (N1) component in the frontal recording sites on the no-go trials in which the animal was not present, interpreted as inhibitive control (Thorpe et al., 1996). Subsequent studies observed a similar pattern of results, a greater early negative divergence in the average waveform for non-animal trials. However, this pattern was not specific to frontal regions, but included temporal and parietal recording sites as well (Antal et al., 2000; Antal et al., 2001). Importantly, in the aforementioned studies (Antal et al., 2000; Antal et al., 2001) the behavioral paradigm was not a go/no-go task. Instead, participants had to make a behavioral response to both target present and target-absent images. Thus these results support the previous findings that the divergence in waveforms is not due to unbalanced motor demands, but due to the task demands (target presence). Moreover, this early negativity was observed in trials in which the target was a vehicle rather than an animal, suggesting the divergence at approximately 150 ms is not due to a specific stimulus category (animal or vehicle), but rather the presence or absence of a target in the image (VanRullen & Thorpe, 2001).

Such studies have led to the general belief that feed-forward processes contribute to the ability to rapidly recognize and correctly categorize scenes based upon their content. However, more recent work has shown that feedback from other areas may also contribute to this response. For instance, Liu and colleagues used intracerebral recordings from epileptic patients to investigate the temporal dynamics, within hundreds of milliseconds, involved when performing object categorization tasks (Liu, Agam, Madsen, & Kreiman, 2009). They observed object category responses as early as 100ms following stimulus presentation. Further support for rapid, early, category recognition was shown when participants made saccades towards the image containing a target within 120-130 ms following stimulus presentation (Kirchner & Thorpe, 2006). Both of these studies suggest that encoding specific characteristics fundamental in scene recognition can occur very rapidly and early in the visual processing stream. Moreover, top-down biasing toward features that are present in the target image may create a template to select for low-level stimulus properties necessary to enable rapid categorization (Delorme, Rousselet, Macé, & Fabre-Thorpe, 2004; Johnson & Olshausen, 2003), yet further processing may be necessary to have a more detailed representation of the scene (Mace, Joubert, Nespoulous, & Fabre-Thorpe, 2009; Rousselet, Macé, Thorpe, & Fabre-Thorpe, 2007). The early negative component could also reflect postsensory processing and be related to a higher level decision process (Johnson & Olshausen, 2005). Thus, the early negativity previously observed at approximately 150 ms may be

due both to early feed-forward processes as well as feedback from higher levels in the visual processing stream.

A number of previous studies have explored the effects of prior adaptation on ERP's, and have generally found that adaptation tends to reduce the response amplitude (Kloth & Schweinberger, 2010; Kovács et al., 2006; Niedeggen & Wist, 1998; Schweinberger, Kloth, & Jenkins, 2007). This attenuation of the waveform has been observed across many stimulus dimensions including, but not limited to motion, eye gaze direction, faces, and body parts. Specifically, adaptation to motion causes a reduction in the amplitude of the N2 component (negativity at 150-200 ms), suggesting decreased neuronal firing and thus reduced sensitivity to motion following prolonged viewing (reviewed in: (Niedeggen & Wist, 1998). Other researchers have found a sizeable reduction in observers' amplitude and an increase in the latency of the N170 component following adaptation to facial and hand stimuli(Kovács et al., 2006). These effects were category-specific such that adaptation to cross-category dimensions (adapt to hand stimuli and test on facial stimuli and vice versa) did not influence the electrophysiological response.

Similar patterns of attenuation of the N170 component were also observed after participants adapted to different directions of eye gaze(Schweinberger et al., 2007). However, in a more recent study (Kloth & Schweinberger, 2010) investigating the neural basis of eye gaze adaptation, it was discovered that the N170 was not susceptible to changes in direction of eye gaze following adaptation, but rather the component was instead sensitive to changes in facial

categories. Further inspection of the waveform revealed that in later components (~250-350 ms), amplitude was reduced when eye gaze was the same direction as the adapt condition.

This latency reflects a special signal in the ERP known as the P300 - a positive deflection that occurs at about 300 ms that is a signature of a "surprising" or unexpected event (Review paper: (Paller, McCarthy, Roessler, Allison, & Wood, 1992; Picton, 1992; Polich & Kok, 1995)). The positive deflection increases in amplitude as the probability of stimulus presentation decreases, and is thus termed the "oddball" response because the response covaries with the infrequency of stimulus presentation. Few studies have used ERP's to investigate how and where in the processing stream visual decisions about medical images are occurring, or how they are impacted by prior adaptation. However, in a recent study by Hope and colleagues (2013), a larger P300 was observed in response to images containing targets (simulated tumors) compared to images without targets (Hope et al., 2013).

Specific Aims

In this dissertation I describe a series of experiments aimed at exploring the effects of adaptation on the perception of medical images. The results of these studies are presented in the following four chapters.

Chapter II investigates how visual adaptation influences the appearance of mammogram images, specifically with regard to how they are normally classified.

In particular, I explore whether adaptation to the characteristic textures defining dense or fatty images affects the perception of the images as dense or fatty.*

Chapter III examines how adaptation to the characteristic, steeper amplitude spectra of medical images alters the perception of image blur and spatial contrast sensitivity. These experiments also explore the relationship between blur perception and the CSF.

Chapter IV tests whether adaptation to the characteristic structure of medical images facilitates the detection of novel or uncharacteristic structures in the images. Specifically, these experiments test whether adaptation improves the ability to search for and locate simulated tumors within the images, and whether these improvements are specific to the class of images (dense vs. fatty) that observers are inspecting and thus adapted to.

Finally, Chapter V explores neural correlates of these adaptation effects by measuring ERP's while observers adapt to mammograms and make visual judgments about them. These experiments parallel the behavioral measurements by testing for electrophysiological signatures of different types of images or for classifying or identifying targets within them.

Together these studies represent the first comprehensive analysis of the influence of a ubiquitous sensory process – adaptation – on the critically important visual judgments involved in interpreting and diagnosing medical images. In the final chapter I discuss future directions and implications of this work for medical image perception.

II. Adaptation aftereffects in the perception of radiological images

In the current study we examined whether the textural differences that distinguish dense or fatty images could be biased by prior adaptation to dense or fatty mammograms. As an initial test of this question, we have focused on demonstrating the existence and magnitude of visual adaptation to these textural properties of mammography images, using tasks to assess adaptation that are straightforward and based on standard experimental paradigms in visual perception. Our focus was also on understanding adaptation to special properties of the image rather than within special populations of observers, and for this reason, we used subjects that are trained for each task, but do not have medical training. Radiologists are highly trained to make an absolute judgment to classify an individual image in terms of how dense or fatty it appears. For our untrained observers this would not be possible, so we instead adopted a procedure in which they were only required to make a relative judgment about which of two presented images appeared more dense or fatty. This allowed us to assess both the extent and form of any possible aftereffects. Our results suggest that there can in fact be profound and rapid aftereffects to the structural properties of medical images, and these have potential implications both for medical image perception and more generally for characterizing how perceptual judgments within unique visual environments might be impacted by routine processes of sensory adaptation.

Materials and Methods

Observers:

Six observers with corrected-to-normal acuity participated in different subsets of experiments. The observers included authors EK and MW (labeled S4 and S6 in figures) and 4 students who were naïve to the purpose of the study. Participation was with written informed consent and followed protocols approved by the University of Nevada, Reno Social Behavioral Institutional Review Board (Office of human research protection).

Apparatus and stimuli:

Stimuli were presented on a calibrated and gamma-corrected Sony 500 PS monitor controlled by a Cambridge Research Systems VSG graphics card. The images were displayed on a gray background on the monitor with the same chromaticity and mean luminance ($\sim$37 cd/m^2).

The stimuli consisted of randomly selected sections taken from a database of normal mammograms (Chen, Abbey, Nosratieh, Lindfors, & Boone, 2012) previously classified with BI-RADS Density scores of "fatty" vs. "dense" (values of 1 or 4), again corresponding to differences in the relative quantities of fat vs. fibroglandular tissue. The sections corresponded to 256 by 256 pixels in the original 2560 by 3328 images, and were constrained to be fully within the breast region of the image. The 8-bit pixel values were rescaled so that the average luminance (37 cd/m^2) and rms contrast (.38) was constant across all images. Sets of these images taken from mammograms classified as dense or

fatty served as the adapting stimuli. For test stimuli, we further created an array of images that varied in finely graded steps between the dense and fatty originals. This was done by averaging the pixel levels from a pair of fatty and dense images, varying the relative weighting to form 101 images spanning the range. An image of +50 corresponded to the original dense image and an image of -50 corresponded to the original fatty image, while image 0 corresponded to an equal mixture of the two (Figure 3). As with the adapting stimuli all test images had the same mean luminance and contrast.

Procedure:

Stimuli were viewed binocularly in a darkened room from 124 cm. At this distance the images subtended 4 deg (~1 arcmin per pixel), and were displayed within fields centered 2.2 deg on the left or right of a central black fixation cross. Specific experiments varied in whether the adaptation was to a single image or sets of images and whether the adapting images were shown in one field or both, as described below. In all cases, observers initially adapted for 60 sec to fatty or dense images, with the adapting field counterbalanced between the left and right sides. Baseline measurements were also taken following adaptation to a uniform field. The adapting stimuli filled the 4-deg displayed window (which was 228 x 228 pixels), but their position within it was randomly jittered every 100 ms over a range of $\pm$16 pixels to avoid local light adaptation.

| Original Fatty | | Intermediate Images | | | | Original Dense |
| 100% Fatty/ 0 % Dense (-50) | 80% Fatty/ 20% Dense (-30) | 65% Fatty/ 35% Dense (-15) | 50%Fatty/ 50% Dense (0) | 35%Fatty/ 65% Dense (15) | 20%Fatty/ 80% Dense (30) | 0%Fatty/ 100% Dense (50) |
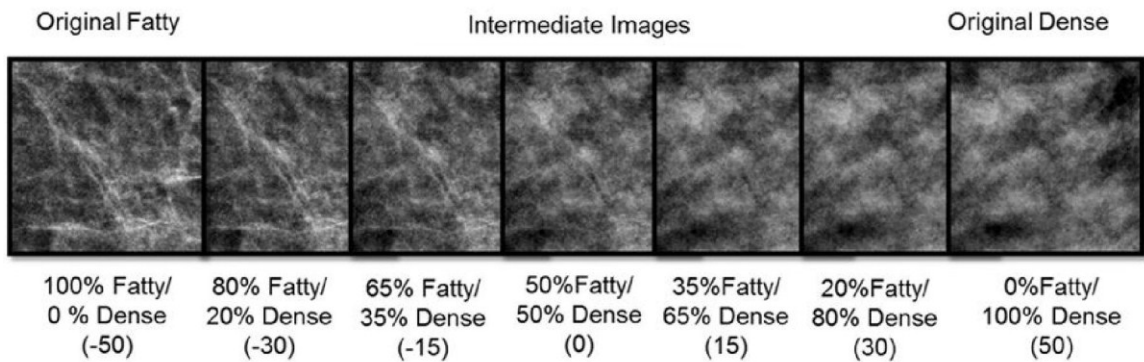
Figure 3. An example of the test stimulus array formed by different weighted averages of a dense and fatty image.

Following adaptation, a probe image was presented in the adapting field(s), and had a level chosen from different points along the fatty-dense array. A matching image with variable level was shown in the opposite field. The probe and match images were displayed simultaneously for 250 ms, and were preceded and followed by a 100 ms gray field. The participants made a 2-alternative response to indicate whether the match image appeared "too fatty" or "too dense" relative to the probe. (The stimulus directions corresponding to these responses could be learned quickly from whether the chosen response caused the two images to converge or diverge in appearance.) Subsequent test stimuli were shown interleaved with 4 sec periods of readaptation, with the array level of the match stimulus varied in a staircase (i.e. an array step toward the dense image if the response was "too fatty" or vice versa). The experiment terminated after 10 reversals of the staircase, and the level at which the two test images appeared to match (i.e. when the two alternative responses were equally likely) was estimated from the mean of the final 6 reversals. Observers made 4 or more repeated measurements for each adapt and test condition in counterbalanced

order, with a different pair of dense/fatty exemplars on each run. The reported results are based on the average of these settings.

Results

Figure 4 provides a simple demonstration of the basic textural aftereffects induced by the dense and fatty images. (A video demonstration is included as supplemental material.) The top pair of images is again two sections from original mammograms classified as dense (left) or fatty (right). The bottom pair is the same on the left and right and was formed by averaging the two top images. Fixating the cross between the top images for several seconds should induce adaptation to the dense or fatty texture within each field. If fixation is quickly shifted to the lower cross, then the physically identical pair may briefly appear different – the right image should appear more dense than the left. Consistent with most adaptation aftereffects, the perceptual change is a "negative aftereffect" because the test image appears less like the adapting image, and results because the adaptation selectively reduces sensitivity to the adapting image (Thompson & Burr, 2009).

To quantify the perceptual shifts, in the first experiment we adapted to both a dense and fatty image in the separate fields as in Figure 4, and then asked observers to adjust the pair of test images with the staircase procedure until they appeared the same. This turned out to be an easy task for observers and also had the advantage that the rms contrast between the two fields remained constant, so that the aftereffects could not be attributed to a simple

aftereffect of apparent contrast. The procedure also had the advantage that it

provided a sensitive probe of any perceptual shift, since the two test fields should

be biased by adaptation in opposite ways, amplifying the appearance difference. To measure this difference, the levels of the two test images were yoked to vary symmetrically around the 50% average, and observers judged whether the right image was more dense or more fatty. That is, a "too fatty" response caused the
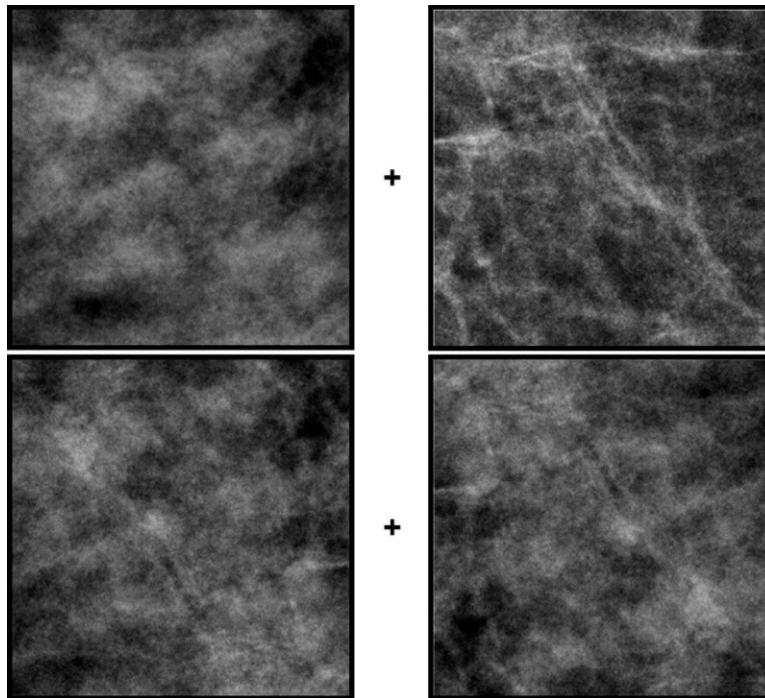
Figure 4. A demonstration of aftereffects induced by adaptation to dense or fatty images. Stare at the cross between the top pair of dense (left) and fatty (right) images for 30 sec and then quickly shift gaze to the cross between the bottom images. These are an average of the two top images, and are physically the same on the left and right (but mirror reversed). However, after adapting the right image should briefly appear more dense.

next displayed pair to be more dense on the right but more fatty on the left.

Figure 5 shows the average settings for 4 observers. Under neutral

adaptation (to a gray screen), the settings approximate a physical match.

However, after adapting to fatty images on the left (and dense on the right), the

test image on the right appeared too fatty, so that the perceived point of equality

was strongly shifted to denser images on the right (and more fatty on the left).
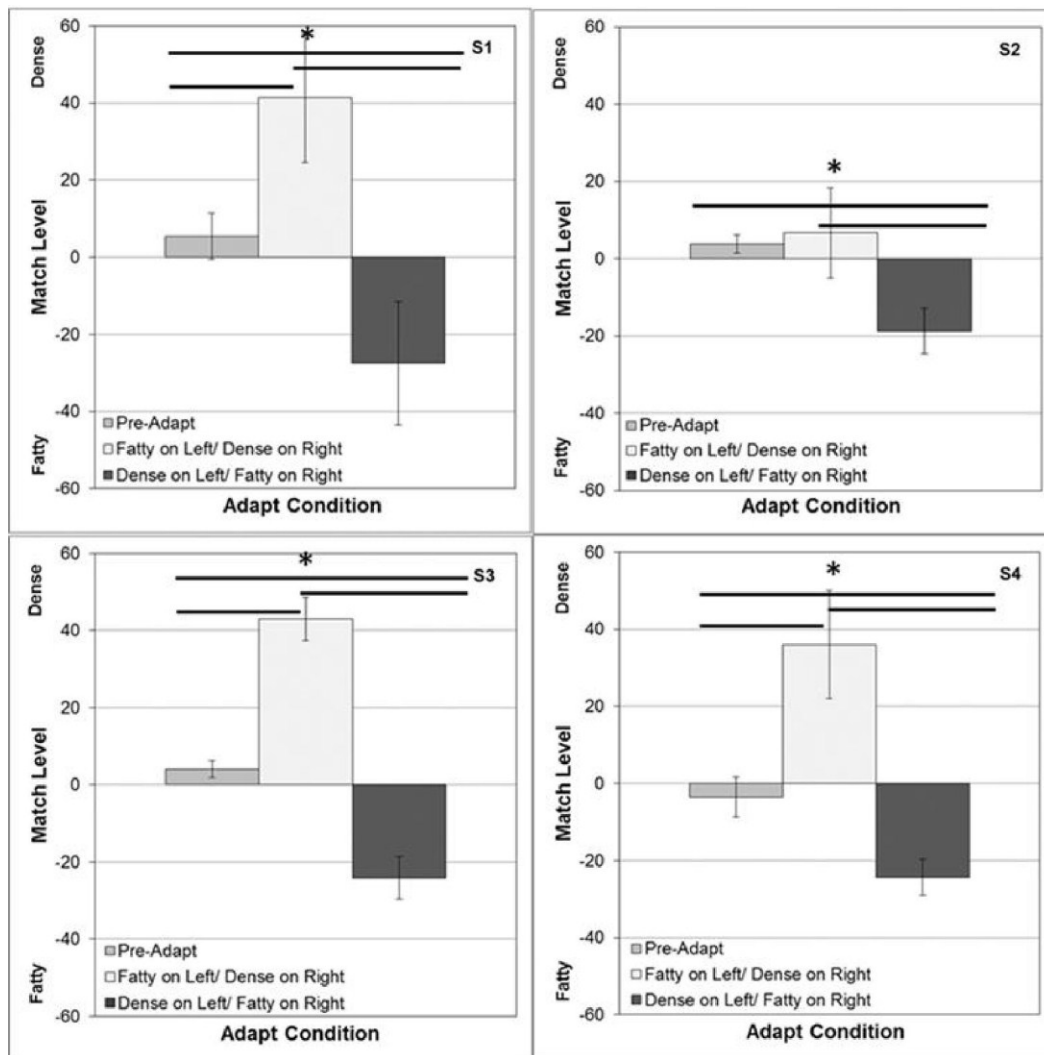
Figure 5. Aftereffects measured with opposite adapting images (dense vs. fatty) displayed in the left and right fields. Each panel shows for one observer the array level of the image on the right that appeared to match the image on the left. Test images were yoked so that when the image was, for example, 40 on the right it was paired with a -40 image on the left. Bars show the mean settings ±1 standard error, when there were no adapting images (left), when the dense image was on the right and fatty on the left (middle), or when the positions were reversed (right). Horizontal lines indicate significant differences in the settings for the 3 conditions.

Not surprisingly, strong complementary aftereffects also occurred when the locations of the two adaptors were switched. Thus in both cases physical differences had to be introduced between the two test images in order to null out the perceptual differences resulting from the adaptation. These aftereffects were significant both relative to neutral adaptation and between the two alternate locations of the adaptors. (For the mean settings across observers, neutral vs. dense $t(6) = -3.37$, $p = .008$; neutral vs. fatty $t(6) = 9.65$, $p < .0001$; dense vs. fatty $t(6) = 6.40$, $p = .0003$).

To further assess the form of the aftereffect, in the second experiment we modified the task so that the adaptation was presented only on the left or right, and so that the probe shown in the adapting field had a constant level. This allowed us to more directly characterize how the appearance of different probe levels were altered by the dense or fatty adaptor since the matching stimulus was no longer also altered by the adaptation (to the extent that the adaptation is specific to the retinal location stimulated, consistent with the opposite aftereffects seen in Figure 5). Figure 6 shows the settings for two observers who matched intermediate probe levels ranging from -30 (80% fatty) to +30 (80% dense). Again, the neutral adapt settings roughly follow the physical match (positive diagonal). After adapting to the fatty images, all of the probe levels appear more dense and thus were equated with a matching level that was physically more dense. Conversely, dense adaptors instead shifted the appearance toward more fatty images, though the magnitude of the aftereffect in the dense case appears weaker. Settings for both observers revealed a highly significant main effect of
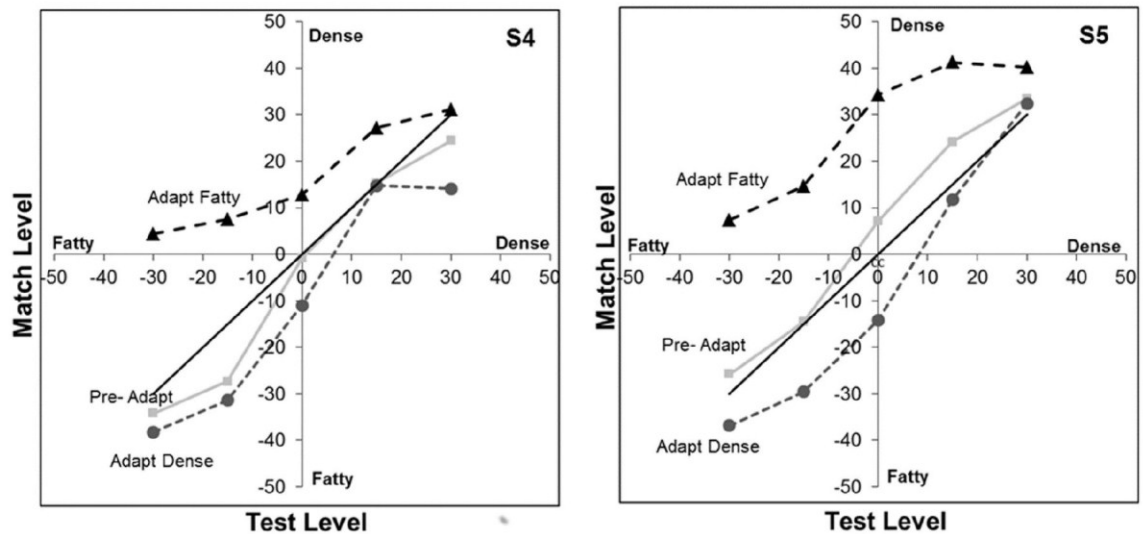
Figure 6 . Aftereffects on different levels of blended fatty vs. dense textures. Curves show the stimulus levels that matched different levels of the test probe before adapting (squares) or after adapting to the fatty (triangles) or dense image (circles). The solid diagonal line corresponds to a physical match. The 2 panels are for 2 observers.

the adapt condition on the image appearance (S1 F(2,45) = 29.5, p<.001; S2 F(2,45) = 58.3, p<.001). However, they differed in whether there was an interaction between the adapt condition and test level (S1 F(8,45) = 1.94, p=.077; S2 F(8, 45), p = .011).

As noted in Methods, the position of the adapt image was jittered during presentation to prevent aftereffects from local light adaptation to the bright and dark regions of the image. However, we next evaluated whether these aftereffects reflected adaptation to the specific pattern of the individual mammogram, or whether they could be also be induced by the dense and fatty textural attributes of the image regardless of which images were carrying those attributes. For this, aftereffects were again assessed for a range of probe levels, but the single adapting image was replaced with a series of dense or fatty

exemplars which were different from the image pair used to construct the test

array. Settings for two observers are shown in Figure 7, and are similar to the

results found for the single adapting images. There is again a significant main

effect of the adapt condition (S1 $F(2, 45) = 21.7$, p<.001; S2 $F(2, 45) = 10.7$, p <

.001) that is stronger for the fatty adaptors and did not interact with the probe

level (S1 $F(8, 45) = 1.53$, p = .18; S2 $F(8, 45) = .35$, p = .94). The similar effects

in this case suggest that adaptation can in fact adjust to the actual textural

properties defining the dense or fatty images, and that these aftereffects can

transfer from one mammogram image to another.
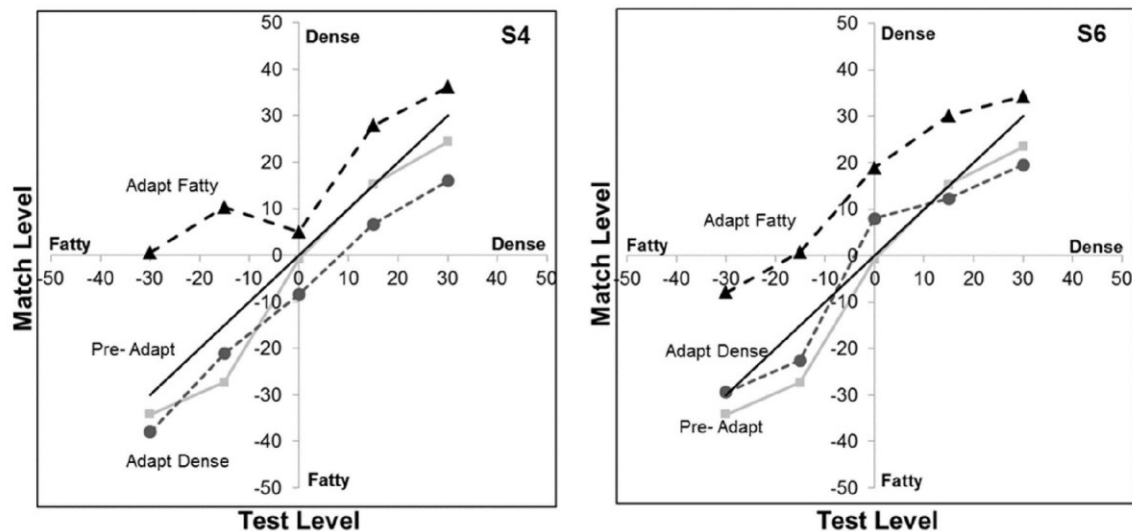
Figure 7. Transfer of the aftereffects across different images. Adaptation was to a sequence of dense or fatty images that differed from the images used to construct the test arrays. Curves show the stimulus levels that matched different levels of the test probe before adapting (squares) or after adapting to the fatty (triangles) or dense image (circles). The solid diagonal line corresponds to a physical match. The 2 panels are for 2 observers.

As a further test of the stimulus properties responsible for the measured

aftereffects, we explored the specific role of the power and phase spectra of the

images. The perceptual differences between most natural images are largely

carried by the differences in phase spectra (Piotrowski & Campbell, 1982),

though differences in the amplitude spectra can also strongly influence which

image is perceived (Tadmor & Tolhurst, 1993). As noted in the introduction,

medical images have steeper power spectra (with power decreasing with

increasing spatial frequency roughly as $p \sim f^{-3}$) than typical natural images ($p \sim$

f^{-2}) (Burgess et al., 2001), and changes in the amplitude spectrum can be a

powerful stimulus for spatial adaptation (M. A. Webster et al., 2002). The slopes

of the power spectra are similar for the fatty and dense images (which had

average spectra of $f^{-2.87}$ sd = .039 and $f^{-2.80}$ sd = .145 respectively), but this

reflects the spectrum averaged across all orientations, and images with the same

slope but different anisotropies (e.g. with astigmatic blur) can also lead to strong

and selective blur aftereffects (L. Sawides et al., 2010). We directly tested the

relative influence of the amplitude and phase spectra on the adaptation by pitting

them against each other. Figure 8 shows a pair of dense and fatty sections after

swapping the phase spectra between the images while retaining the power

spectrum of each image. The identity of each more closely follows the phase

spectrum. We used these swapped images to similarly test whether the direction

of the textural aftereffect followed the power or the phase spectrum. This

experiment used the same procedures and images as in the double-adapt

paradigm of Figure 5, except that the adapt image pairs were replaced with the

hybrid images as in Figure 8. Consistent with the perceptual differences, the sign

of the aftereffects remained tied to the phase spectrum for 3 observers (with no

significant aftereffect either way for a fourth observer), again suggesting that it is

primarily an adaptation to the textural attributes of the images (Figure 9). In the

preceding conditions the adapting images were always dense or fatty and thus at

the extremes of the image array, while the probe images were at intermediate

levels. The results

were consistent with adaptation to either mammogram type causing test images

to appear less like the image the observer was previously adapted to (though
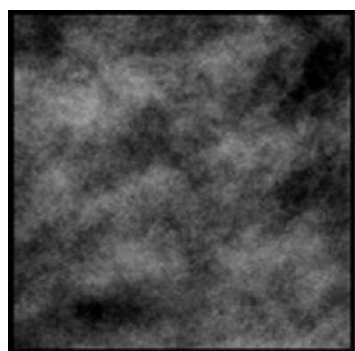
Figure 8. Examples of image pairs before or after swapping the power spectra. The top pair shows the original images, while the bottom pair has the power spectrum from the image above it but the phase spectrum of the second original.
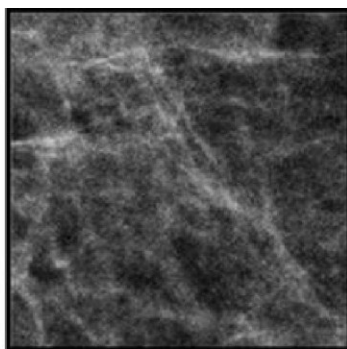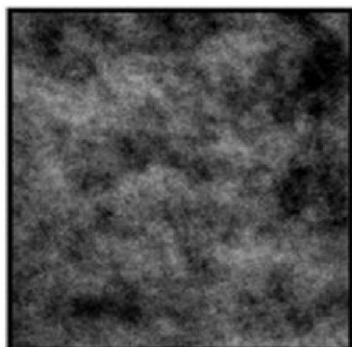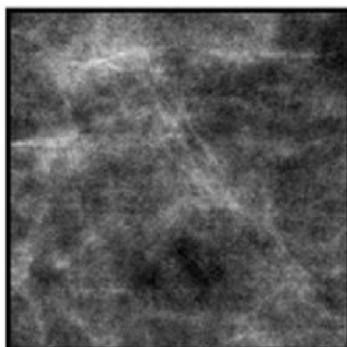
again these aftereffects were weaker for the dense adaptors). However, what happens to the appearance of the adapting image itself? Does its perceived texture change or do we simply become less sensitive to that texture? These questions have been of general importance to evaluate the nature of the perceptual changes

resulting from adaptation (Rhodes et al., 2005; M. A. Webster & MacLeod, 2011).

For some dimensions (e.g. color) the stimulus appears weaker (e.g. less saturated) with prolonged viewing, consistent with a more global renormalization of the response so that the adapt stimulus appears more neutral (e.g. gray). For other attributes (e.g. size) the adapt level does not appear to change while both
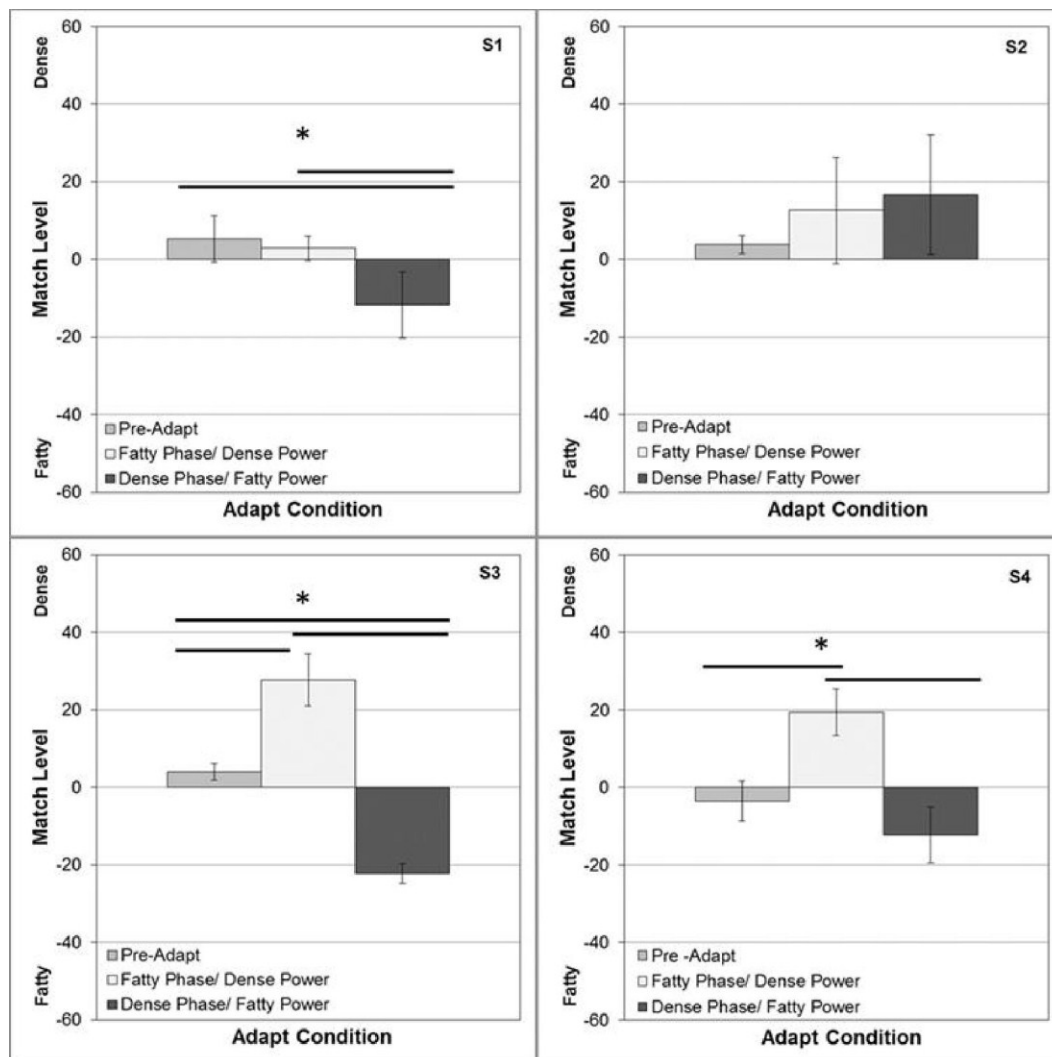
Figure 9. Aftereffects for the phase-swapped images. Aftereffects were tested as in Figure 5. Bars show the mean settings +1 standard error, when there were no prior adapting images (left), when the image with the fatty phase and dense power was on the left and the image with the dense phase and fatty power was on the right (middle), or when the positions were reversed (right). Horizontal lines indicate significant differences in the settings for the 3 conditions.

higher or lower levels appear biased away from the adapting level, consistent

with a more local sensitivity change around the adapting level. To examine this,

we modified the experiment so that the probe image now equaled the adapting

image, and so that the effects were assessed not only for the original dense and
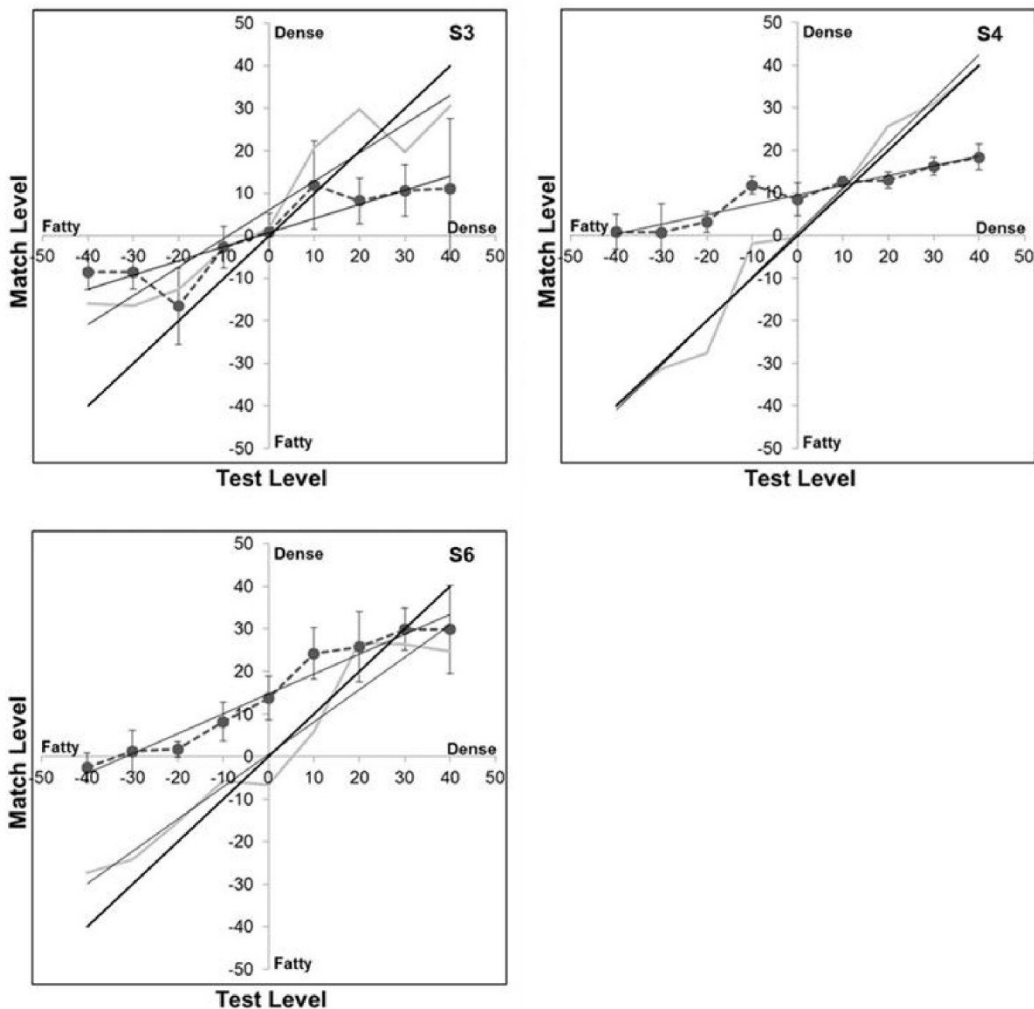
Figure 10. Changes in the appearance of the adapting image. Curves plot the matches made to different test levels before (gray line) or after (connected circles) adapting to the same level. Thin solid lines plot the linear regression lines. Thick solid line corresponds to the physical match. Panels plot the results for 3 observers.

fatty images but also for intermediate adapting levels. If the adapt image was not altered in appearance, then no aftereffects should have been observed under this condition. Instead, the matches were again strongly biased (Figure 10). Specifically, adaptation to denser images caused them to appear less dense, and adaptation to fatty images caused them to appear less fatty. In the results this is indicated by the reduction in the slope of the match settings for the different adapt levels (since these levels now appear more similar or intermediate), and these slope changes were significant (e.g. for the mean settings across observers $F(1,50) = 5.015$, $p = .030$). Notably, for two of the three observers, the appearance biases were not centered on the balanced average of the fatty and dense images but were instead biased toward moderately denser images (so that these moderately denser images were thus closer to the "neutral" point for the arbitrary texture dimension defining the stimulus array). This is again consistent with a weaker aftereffect for the dense images since by this criterion they differed less from the neutral stimulus and thus had a lower effective "contrast" along the dimension.

Discussion

In summary, we have shown that brief exposures to different categories of mammogram images can lead to robust aftereffects in the appearance of the images. This has both general implications for adaptation and texture perception, and specific implications for the potential influence of adaptation on the visual perception of medical images. We consider these in turn.

As noted at the outset, the visual system can selectively adapt to a wide array of image properties from simple features to high-level attributes, and these adjustments can lead to very salient changes in appearance. The fact that adaptation could occur for properties of medical images is thus not surprising. However, it is important as a further illustration that adaptation can be manifest for the types of images and visual tasks that at least some observers are routinely exposed to, and thus as an example of the pervasive influence of adaptation on our perception (M. A. Webster, 2011a). Our results show that strong aftereffects can be induced by the differences that distinguish fatty vs. dense images, and suggest that these reflect the textural differences between the two image classes. Specifically, the aftereffects could not be accounted for by differences in contrast (which was nominally equated in the images) or power spectra (which were similar across the images and which did not predict the aftereffects; Figure 9). Instead, they followed the phase spectrum of the images, which also predicted the images' appearance. Moreover, similar aftereffects occurred when observers were adapted to fatty or dense exemplars that were not the same images used in the test array (Figure 7). This indicates that the aftereffects could be induced by the spatial structure defining the dense or fatty categories separately from the identity of a specific image.

Aftereffects on the appearance of visual texture have been demonstrated previously. For example, the perceived density of a dot texture can be biased by prior adaptation to a field with sparse or cluttered elements (F. H. Durgin, 2008; F. H. Durgin & Proffitt, 1996). These density aftereffects occur for artificial and

naturalistic textures, and as we found cannot be accounted for by differences in

power spectra (F.H. Durgin & Huk, 1997). A recent study also found adaptation

to the "regularity" of textures (e.g. arrays of elements with uniform or random

spacing)(Ouhnana, Bell, Morgan. M.J., Solomon, & Kingdom, 2013). Similarly,

surface properties such as whether a material appears glossy or matte can be

strongly biased by adaptation to the image statistics tied to these perceived

attributes (Motoyoshi, Nishida, Sharan, & Adelson, 2007). However, the effects of

adaptation on texture perception are not well understood. One surprising finding

with the images we studied is that the perceived texture of the adapting image

itself changed with exposure – both fatty and dense images appeared less fatty

or dense following adaptation (Figure 10).This is reminiscent of the perceptual

changes that occur for attributes like color or facial configurations, which look

less "saturated" with adaptation (M. A. Webster & MacLeod, 2011). These have

typically been accounted for by assuming that the underlying response changes

occur within visual mechanisms that are broadly tuned for the stimulus

dimension, and potentially as part of a norm-based code in which the stimulus is

represented by how it differs from the norm (Rhodes et al., 2005; M. A. Webster

& MacLeod, 2011). By such accounts the aftereffects reflect a renormalization of

the coding dimension so that the adapting level appears more neutral. Obviously,

it is unclear what the actual visual coding dimensions are that underlie our ability

to discriminate an arbitrary stimulus variation like fatty vs. dense images.

However, whatever they are, they intriguingly behave as if they have a coding

norm, and moreover adaptation can be used as a potential tool for defining this

norm. In particular, the image level that does not change in appearance with adaptation is a plausible candidate for the neutral point in the continuum, since this is presumably the stimulus level to which the visual system is already adapted and thus "in balance" for (M. A. Webster & Leonard, 2008). In Figure 10, this corresponds to the point at which the pre- and post-adapt settings intersect. As noted, these are biased toward denser images (relative to the stimulus averages we created), and consistent with this, dense images also appeared to be less effective as adaptors. This predicts that image textures that are classified as dense might effectively be less "saturated" and thus possibly less visually salient than fatty textures, again because they are closer to the neutral point.

Before discussing potential implications of these aftereffects for the visual evaluation of medical images, several limitations of our study should be noted. First, as noted in the Introduction we did not test radiologists but instead untrained observers. There is no reason to think that observers are less susceptible to adapt to images that they have more familiarity with, and in fact the converse is possible. Yet as discussed below, the dynamics or form of the aftereffects could be affected by extensive experience. Second, our stimuli were hybrids formed by blending actual images, and may not suitably capture the properties of images that are rated as intermediate on the BI-RADS scale. Also, because our observers could not use this scale, it remains to be seen whether the adaptation could be strong enough to significantly alter the classification of the image. Finally, the adapting procedure we used was designed to generate strong and stable states of adaptation for specific properties of the images, and is

very different from the sequence of stimulus exposures that might occur during a radiological reading. Thus the degree to which adaptation might impact performance in an actual screening remains to be explored.

Nevertheless, our results show that observers can strongly adapt to characteristics that distinguish mammogram images, and thus suggest that pattern-selective adaptation is potentially a significant but previously unrecognized factor affecting the perception and interpretation of medical images. In the simplest scenario, the aftereffects predict that the current image may tend to look less like the images viewed previously, giving rise to potential order effects in how images are evaluated. Moreover, our findings also point to the potential for changes in the perception of the current image itself depending on the duration of the inspection. Again, whether these turn out to play a measurable role in actual radiological settings is a question for future research, but could be explored by varying the sequence and timing of the image sets.

There may also be positive consequences of adaptation. The functional benefits of pattern adaptation have remained difficult to demonstrate (C. W. Clifford et al., 2007; Kohn, 2007; M. A. Webster, 2011a). One prevalent account is that adaptation might enhance discrimination of stimuli similar to the adaptor by centering neural responses at the adapting level, though evidence for this is limited. Another account is that it allows the visual system to predict and thus discount the expected properties of the environment so that neural and perceptual resources can be devoted to unexpected properties. Interestingly, this in some ways mirrors the task confronting the radiologist, who must search

the image to identify anomalous features. There is in fact some evidence that adaptation can enhance the salience of statistical outliers in stimulus distributions (McDermott et al., 2010; Wissig et al., 2013), and thus could in theory aid the radiologist by making rarer features in the image more perceptually conspicuous.

Finally, the context of medical image perception provides unique opportunities for exploring a number of unanswered questions about the nature of visual adaptation. Again, this is because the images themselves have "unnatural" but well characterized statistics and because radiologists have very extensive exposure to them. This allows for examining unresolved issues such how adaptation interacts with other experience-dependent processes such as perceptual learning (Harris, Gliksberg, & Sagi, 2012) or visual expertise, and how the processes of adaptation operate over much longer timescales than are normally possible in the lab. Recent studies have suggested that the dynamics of adaptation extend over multiple durations (Bao & Engel, 2012; Belmore & Shevell, 2010; Delahunt, Webster, Ma, & Werner, 2004; Kording, Tenenbaum, & Shadmehr, 2007; Neitz, Carroll, Yamauchi, Neitz, & Williams, 2002; Vul, Krizay, & MacLeod, 2008), and that even the form of the response changes might vary with the length of exposure (Kwon, Legge, Fang, Cheong, & He, 2009). A further possibility is that the visual system might exhibit context-dependent adaptation so that it can store and rapidly engage different response states appropriate for different environments (Yehezkel, Sagi, Sterkin, Belkin, & Polat, 2010). That is, an observer like a radiologist may be able to perceptually adjust more quickly to a context they have previously encountered. Because radiologists have had very

long-term exposure to types of images that untrained observers rarely see, measurements of the nature of their own adaptation to medical images could also help reveal functional consequences of adaptation that are generally hidden in typical experimental paradigms or populations, either because the performance benefits require long adapting periods to emerge or because they are hidden in studies of natural images because observers are already expert (and thus there is no "untrained" group for comparison) (M.A. Webster & Juricevic, 2013).

III. Adaptation to the amplitude spectra of medical images

As previously emphasized, radiological images often have visual properties that are distinct from natural images and which could impact visual performance. One well-known difference is in their amplitude spectrum, which plots the amount of contrast at different scales or spatial frequencies in the images. Natural images have a characteristic amplitude spectrum in which contrast varies inversely with spatial frequency, or as 1/f (e.g. so that contrast is halved each time the frequency doubles). On a log-amplitude vs. log-frequency plot this relationship results in a line with a slope of -1. Images like mammograms instead have a steeper spectrum (Burgess et al., 2001), in which energy falls off more rapidly as frequency increases. Typically this follows a function like $1/f^{1.5}$ or a line with a slope of 1.5 on a log-log plot. (This structure is also often characterized in terms of the power spectrum, which is the square of the

amplitude spectrum. Thus natural images tend to have a power spectrum of -2, while mammograms are closer to -3 (Burgess et al., 2001; Burgess et al., 1997).

Visually, a steeper power spectrum corresponds to less visible fine detail and thus the images appear more blurred. Blur is a fundamental and highly salient attribute of image quality, and a property of images that the visual system readily adapts to (Elliott et al., 2011; E Kompaniez, Sawides, Marcos, & Webster, 2013; Lucie Sawides, de Gracia, Dorronsoro, Webster, & Marcos, 2011; Vera-Diaz et al., 2010; M. A. Webster et al., 2002; Yehezkel et al., 2010). This predicts that the physical blur in medical images should induce strong changes in the state of blur adaptation. In the following experiments, these blur aftereffects are assessed when observers are adapted to mammograms, and are examined in two ways. First, we investigate whether adaptation to mammograms alters the perceived blur in images. Second, we investigate how the adaptation affects the spatial sensitivity of the visual system. This sensitivity is characterized by the contrast sensitivity function (CSF), which measures the contrast threshold for detecting a stimulus as a function of its spatial frequency. The CSF is a standard tool for predicting visibility and performance with images including medical images. Thus how the CSF might change with adaptation is important for evaluating the consequences of adaptation for medical image perception.

Materials and Methods

Observers:

Five observers with corrected-to-normal acuity participated in different subsets of experiments. The observers included authors EK and 4 students who were naïve to the purpose of the study. Participation was with written informed consent and followed protocols approved by the University of Nevada, Reno Social Behavioral Institutional Review Board.

Apparatus and stimuli:

Stimuli were presented on a calibrated and gamma-corrected Sony 500 PS monitor controlled by a Cambridge Research Systems VSG graphics card. The images were displayed on a gray background on the monitor with the same chromaticity and mean luminance (~37 cd/m^2).

The stimuli consisted of randomly selected sections taken from a database of normal mammograms (Chen et al., 2012) previously classified with BI-RADS Density scores of "fatty" vs. "dense" (values of 1 or 4), again corresponding to differences in the relative quantities of fat vs. fibroglandular tissue. The sections corresponded to 256 by 256 pixels within the original 2560 by 3328 images, and were constrained to be fully within the breast region of the image. The 8-bit pixel values were rescaled so that the average luminance (37 cd/m^2) and rms contrast (.38) was constant across all images. In the suprathreshold task we examined adaptation to variations in the slope of the amplitude spectra, similar to the study of blur aftereffects by Webster et al. (2002) (M. A. Webster et al., 2002). The adapting stimuli (Figure 11) consisted of the original mammogram image (e.g. with a slope of ~-1.4) and four versions of

the images filtered to have shallower slopes (-1.25, -1, -.75, and -.5). Note again that -1 corresponded to a "natural" or perceptually focused slope while shallower slopes correspond to images that in most natural images would appear overly sharpened. For test stimuli, we created an array of images that varied the level of blur/sharp in finely graded steps to create an array that consisted of mammogram images filtered to be more blurry or sharp relative to the original scan. Both the adapt and test images were created by multiplying the original amplitude at each frequency (f) by f^{α}, with α varied from -0.5 to +0.5 to form 101 images spanning the range. As with the adapting stimuli all test images had the same mean luminance and contrast.

Procedure:

1. Suprathreshold Matches

Stimuli were viewed binocularly in a darkened room from 124 cm. At this distance the images subtended 4 deg (~1 arcmin per pixel), and were displayed within fields centered 2.2 deg on the left or right of a central black fixation cross. In all cases, observers initially adapted for 60 sec to both the original mammogram image and to those filtered to have shallower slopes displayed in separate fields, with the adapting field counterbalanced between the left and right sides. Baseline measurements were also taken following adaptation to a uniform gray field. The adapting stimuli filled the 4-deg displayed window (which was 228 x 228 pixels), but their position within it was randomly jittered every 100 ms over a range of $\pm$16 pixels to avoid local light adaptation.
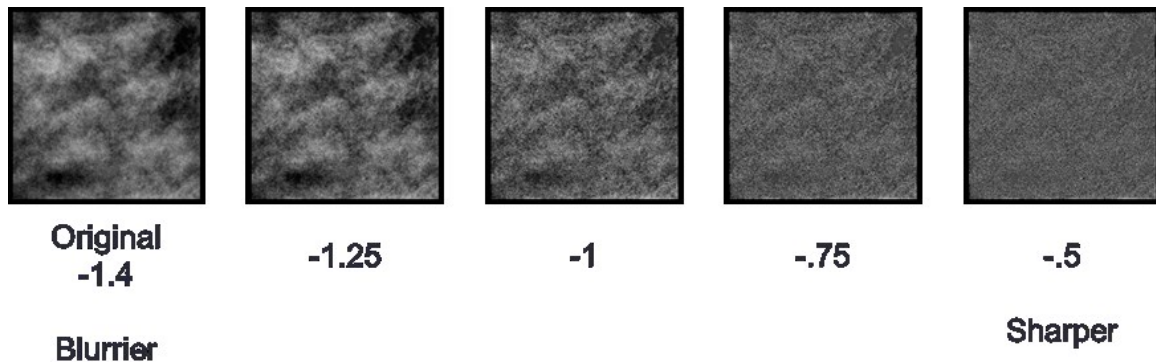
Figure 11. Adapting stimuli consisting of the original mammogram image and mammogram images filtered to have shallower slopes and thus appear sharper relative to the original image.

Judging when a noise-like image like a mammogram appears in focus is a perceptually difficult task, since it requires comparing the image to some internal reference for subjective focus for an image that does not have distinct structure or features such as well-defined edges. To test for blur aftereffects, we instead used a relative judgment in which observers adapted to both a blurred and sharpened image in the separate fields as shown in Figure 11, and then adjust a pair of test images using a staircase procedure until they appeared the same. As discussed in the previous chapter, this design had the advantage that the rms contrast between the two fields remained constant, so that the aftereffects could not be attributed to a simple aftereffect of apparent contrast. The procedure also had the advantage that it provided a sensitive probe of any perceptual shift, since the two test fields should be biased by adaptation in opposite ways, amplifying the appearance difference. To measure this difference, the levels of the two test images were yoked to vary symmetrically around the setting corresponding to a slope of -1 and thus focused in appearance (match level 0). Participants judged whether the right image was more blurred or sharp relative to the left image. That

is, a "blurred" response caused the next displayed pair to be more sharpened on the right but more blurred on the left. (The stimulus directions corresponding to these responses could be learned quickly from whether the chosen response caused the two images to converge or diverge in appearance.)

The test images were displayed simultaneously for 250 ms, and were preceded and followed by a 100 ms gray field. Subsequent test stimuli were shown interleaved with 4 sec periods of readaptation. The experiment terminated after 10 reversals of the staircase, and the level at which the two test images appeared to match (i.e. when the two alternative responses were equally likely) was estimated from the mean of the final 6 reversals. Observers made 4 or more repeated measurements for each adapt and test condition in counterbalanced order, with a different pair of blurred/sharpened exemplars on each run. The reported results are based on the average of these settings.

2. Contrast Thresholds

To examine how adaptation influenced contrast thresholds, stimuli were viewed binocularly in a darkened room from 200 cm. At this distance the images subtended 5 deg and were displayed in the center of the screen. Observers initially adapted for 120 seconds to an array of images drawn from one of three sets: the original dense mammogram images, the same images filtered to slope of ~-1, or a gray field (used to measure threshold contrast sensitivity prior to adaptation). The adapting images were cycled every 250 ms to avoid local light adaptation. After the initial adaptation period there was a 250 ms interstimulus

interval (ISI), a test grating of fixed frequency was displayed for 500 ms, and the

participant signaled with a button press whether the grating was oriented at either

45 deg or 135 deg. This was followed by a 250 ms ISI and then a readaptation

period of 4 sec. Contrast was varied in a 3-down 1-up staircase with the run

terminated after 11 reversals. Thresholds were calculated from the mean of the

final 8 reversals. Grating spatial frequency remained constant during a run and

ranged from 0.5 to 16 c/deg in one-octave steps across runs. Four runs were

repeated for each adapting condition, and the reported results are based on the

average of these settings.

Results

1. Suprathreshold Matches

Figure 12 and 13 show average settings for 5 participants. The figures plot for

each adaptation condition (dense or fatty) the change in perceived blur/focus

arising after prolonged viewing of the original scans. When adapting to a gray

screen (baseline condition), observers' settings were perceptually focused. Thus

with no adaptation to dense (fatty) images observers were able to accurately

judge the level of focus within the filtered mammograms. However, after adapting

to the original dense image on the left and a sharpened version of the image on

the right, the subsequent test images on the right appeared too blurred and on

the left too sharp. Thus, the perceived point of equality was biased toward

sharpened settings on the left and vice versa on the right. The graphs plot the

difference that needed to be introduced in the left image to null out the perceptual differences introduced following adaptation.

For the dense images, settings were significantly biased in the sharpened direction

Figure 12. Aftereffects for the filtered mammogram images (original unfiltered vs. filtered) displayed in the left and right fields. Each bar shows the array level of the image on the right that appeared to match the image on the left (original dense image). Test images were yoked so that when the image was, for example, 40 on the right it was paired with a -40 image on the left. Bars show the mean settings ±1 standard error. Horizontal lines indicate significant differences in the settings of the filtered images relative to baseline (no adapt) condition.

compared to the neutral (gray field) adaptation ($F_{(2, 20)} = 6.124$, $p < .01$). The shifts were in the same direction for the fatty images, though in this case the differences were not significant, possibly because observers were less reliable in making the relative blur judgments with the fatty images.
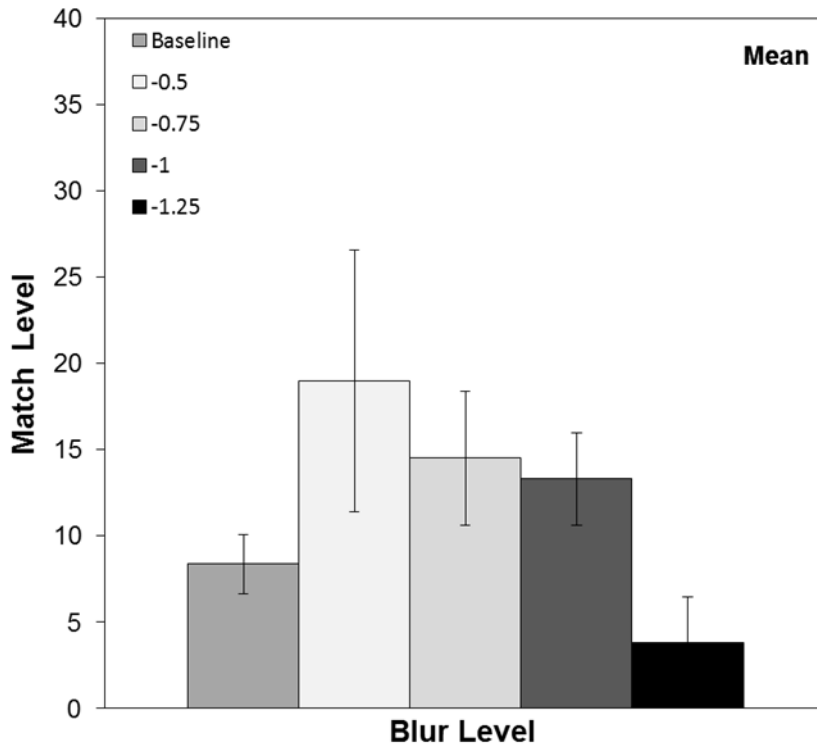
Figure 13. Aftereffects for the filtered mammogram images. Aftereffects were tested as in Figure 12. Bars show the mean settings +1 standard error, after adapting to fatty images.

2. Contrast Thresholds

Figure 14 shows how adaptation to the mammogram images instead affected threshold contrast sensitivity. Gray squares plot the CSF for neutral (gray field) adaptation, while filled circles represent the CSF following adaptation to mammogram images and filled triangles represent the CSF following adaptation to the filtered scans with a slope of – 1 (perceptually focused). The CSF shows typical bandpass tuning with peak sensitivity under neutral adaptation to ~2 – 4 c/deg. In contrast, adaptation to both the original mammograms and those filtered to a 1/f spectrum show a selective loss in sensitivity at low to medium spatial frequencies. As a result, the CSF more clearly peaks at ~ 4 c/deg, and sensitivity to higher frequencies remained largely unaffected by the adaptation. For the mean settings across

observers there was a main effect of spatial frequency ($F_{(5, 20)}$ = 5.161, p = .003, and a significant effect of adaptation condition, $F_{(2, 8)}$ = 5.178, p = .036).
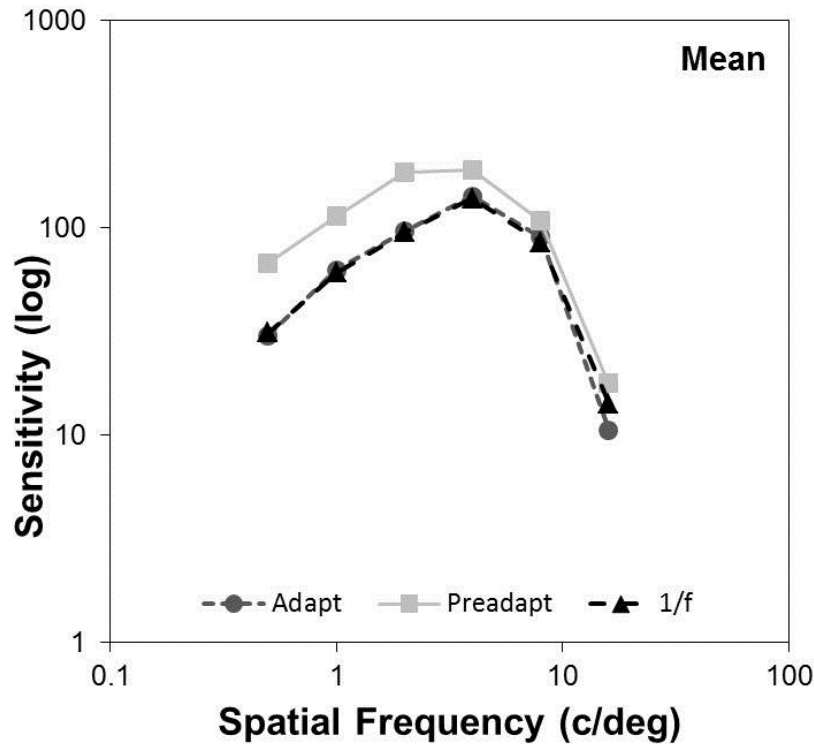
Figure 14. Average CSF following neutral (gray field) adaptation (light gray squares), adaptation to the original mammogram scans (dark gray circles) and adaptation to mammogram images filtered to have a slope of -1 (black triangles). For the mean settings across observers: main effect of spatial frequency $F_{(5, 20)}$ = 5.161, p = .003 and a significant effect of adaptation condition, $F_{(2, 8)}$ = 5.178, p = .036.

Discussion

Our results reveal that adaptation to the characteristic amplitude spectra of mammogram images induces characteristic changes in suprathreshold blur perception and in threshold contrast sensitivity. We consider each of these effects in turn and then consider how the two aftereffects are related.

Blur aftereffects of the kind we observed have now been widely studied and occur both when images themselves are blurred or when blur is introduced by the optical aberrations of the eye (Elliott, Georgeson & Webster, 2011, Vera-

Diaz, Woods & Peli, 2010, Webster, Georgeson & Webster, 2002; George &

Rosenfield, 2004, Mon-Williams, Tresilian, Strang, Kochhar & Wann, 1998,

Pesudovs & Brennan, 1993, Rajeev & Metha, 2010, Rosenfield & Gilmartin,

1999; Sawides, Marcos, Ravikumar, Thibos, Bradley & Webster, 2010, Yehezkel,

Sagi, Sterkin, Belkin & Polat, 2010). In fact it is likely that this adaptation

functions to calibrate spatial vision and subjective image focus by discounting the

retinal image blur induced by the eye's optics (Elliott et al., 2011 (Artal, Chen,

Fernandez, Singer, Manzanera & Williams, 2004, Sawides, de Gracia,

Dorronsoro, Webster & Marcos, 2011a, Sawides, de Gracia, Dorronsoro,

Webster & Marcos, 2011b). In most situations it is the characteristics of the

observer that is the primary source of blur – i.e. their optical errors. Again, this is

because the world typically has constrained spatial statistics such that the

amplitude spectra of most scenes fall as roughly 1/f (Field & Brady, 1997) (and

because the optical quality of eyes by comparison varies markedly). Our results

with mammograms illustrate an important case where the environmental

variations are large enough to alter the state of blur adaptation. That is, the

"unnatural" visual world that mammograms present through their steepened

amplitude spectra is sufficient to recalibrate spatial vision so that the perception

of blur and image focus is significantly altered.

Our results also parallel previous findings in showing that adaptation to

images with the biased spectra characteristic of natural images alters the CSF by

selectively reducing sensitivity to lower spatial frequencies (Bex et al., 2009;

Sharpee et al., 2006; M. A. Webster & Miyahara, 1997). Again, this is important

because the CSF is widely used to predict visibility and visual performance, and well recognized that it is important to use a measure of the CSF that is appropriate for the viewing conditions of the observer. For example, the CSF varies widely with factors such as mean luminance, temporal frequency, or location in the visual field(De Valois & De Valois, 1990). The present results confirm that another significant factor is the observer's state of contrast adaptation.

Interestingly, both our measurements and previous studies have found that the effects of adaptation on CSF are not strongly dependent on the precise slope of the adapting spectra. In particular, as also reported by Webster and Miyahara (1997), the threshold changes were virtually identical whether observers were adapted to a spectral slope of -1 or -1.5, and it was only for larger deviations that substantially different CSFs may emerge (M. A. Webster & Miyahara, 1997). In this regard, the visual world of mammograms is not unnatural – for it appears to induce similar adaptation states.

But how can adaptation to different spectral slopes alter the appearance of fine detail in the image (blur aftereffects) when it does not seem to alter the sensitivity to fine detail (as measured by the contrast sensitivity function)? The answer to this question is complex but is likely to reflect the complex relationship between threshold sensitivity and suprathreshold appearance. The actual basis of blur perception in the visual system is in fact poorly understood - it is not clear whether blur is coded as feature that is present in images (e.g. the fuzziness of edges) vs. one that is absent (e.g. inability to see expected details). In the former

case, it is also unknown whether the attribute of blur is coded as an explicit image feature or implicitly by the pattern of energy across different spatial scales. What our results do support is evidence that subjective judgments of focus and how these are adapted cannot be predicted from the thresholds limiting spatial vision, even though these thresholds do predict blur discrimination (Watson & Ahumada, 2011). There are several arguments for these differences (M. Webster, Mizokami, Svec, & Elliott, 2006). However, among the most telling that our results demonstrate, is that adapting to an image that is physically in focus induces a large change in the CSF by selectively reducing sensitivity to lower frequencies, but does not cause images themselves to appear sharper.

Regardless of the basis for these different aftereffects, we have shown that they are manifest in predictable ways in the medical images that radiologists are routinely exposed to. Thus again this suggests that adaptation is an important factor in understanding the how medical images are perceived.

IV. Adaptation and visual search in medical images

Radiologists face the visually challenging task of searching for diagnostically important information within medical images. Often this involves detecting anomalies or suspicious features within images that have complex and noisy background characteristics. Moreover, these characteristics often reflect unnatural image statistics that are therefore themselves "anomolous" relative to the normal visual diet of an observer. Visual training for medical image diagnosis is obviously fundamentally important for developing the requisite skills for reading

and interpreting the images. In this study, we investigated a form of short-term "learning" based on visual adaptation. One functional account of adaptation is that it serves to highlight the salience of novel stimulus properties by discounting or reducing the salience of ambient or expected properties of the images. In support of this, recent studies have found that prior adaptation to a set of colors (McDermott et al., 2010) or orientations (Kohn, 2007) can increase the efficiency of searching for a novel color or orientation.

In the current study, we investigated if adaptation could enhance the salience of a target in medical images, such as searching for a lesion or tumor in radiological scans. As our previous findings revealed, adaptation to medical images produces robust and rapid aftereffects in the perceived texture of mammogram images (E. Kompaniez, Abbey, Boone, & Webster, 2013). Here we investigate whether this adaptation also influences the ability to detect information within the mammograms. Gaussian targets simulating lesions were added to the images, and a visual search task was used to examine whether the salience of these targets could be enhanced by prior adaptation to the mammogram scans. The results of these studies suggest that visual salience and search efficiency can be heightened when observers are first adapted to the backgrounds they are searching on, perhaps because this adaptation allows observers to more effectively suppress the structure of the background.
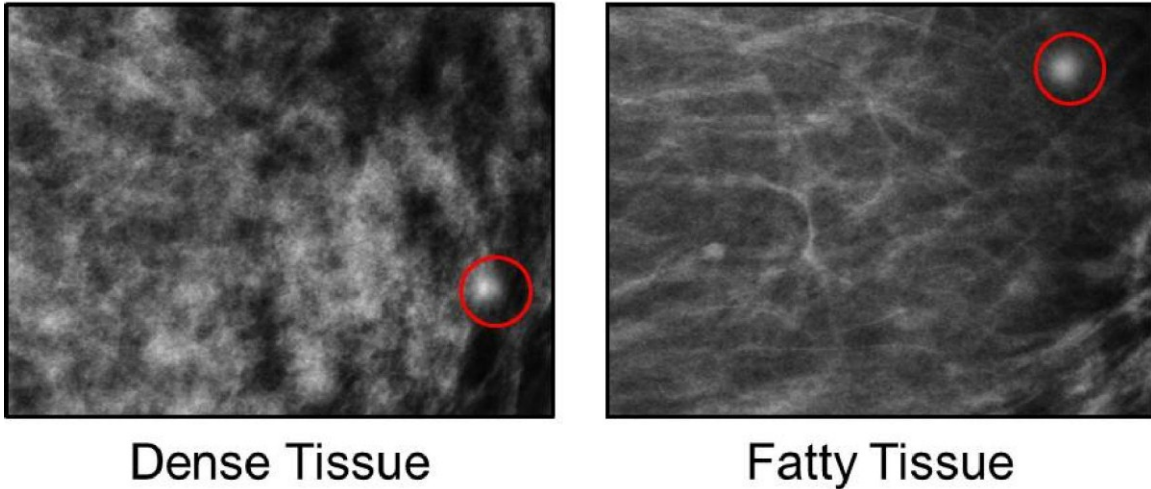
Figure 15. Random sections taken from within previously classified mammogram images with simulated lesion added (test stimuli).

Materials and Methods

Observers:

Ten observers with corrected-to-normal acuity participated in the experiments. The observers included authors EK and MW and 8 students who were naïve to the purpose of the study. Participation was with written informed consent and followed protocols approved by the university's Institutional Review Board.

Apparatus and stimuli:

Stimuli were presented on a calibrated and gamma-corrected Sony 500 PS monitor controlled by a Cambridge Research Systems VSG graphics card. The stimuli consisted of randomly selected sections taken from a database of normal

mammograms previously classified with BIRADS Density scores of "fatty" vs.

"dense," again corresponding to differences in the relative quantities of fat vs.

fibroglandular tissue. The sections corresponded to 800 by 600 pixels in the

original 2560 by 3328 images, and were constrained to be fully within the breast

region of the image; see Figure 15. Sets of these images taken from

mammograms classified as dense or fatty served as the adapting stimuli. For the

test stimuli, we used similar random sections taken from previously classified

mammograms. These were all taken from different images than the adapt

images, and consisted of 20 images from mammograms classified as dense and

20 images classified as fatty. For each, targets were added to simulate the

presence of a lesion. These corresponded to incremental Gaussian spots (sd =

.18 deg), superimposed by adding the spot's luminance to the background

(Figure 15). The location of the target was chosen randomly with the constraint

that it did not fall within the .55 deg to the left or right of the center of the

background and thus could be readily localized to the left or right side of the

image. Finally, target contrast was varied in separate images over 5 levels so

that detection varied from easy to difficult (Figure 16).

Procedure:

Observers viewed the display binocularly in a darkened room from a distance of

260 cm, at which the screen subtended 6.6 by 8.75 deg. In the pre-adapt

conditions, observers initially adapted to a uniform gray field for 30 seconds
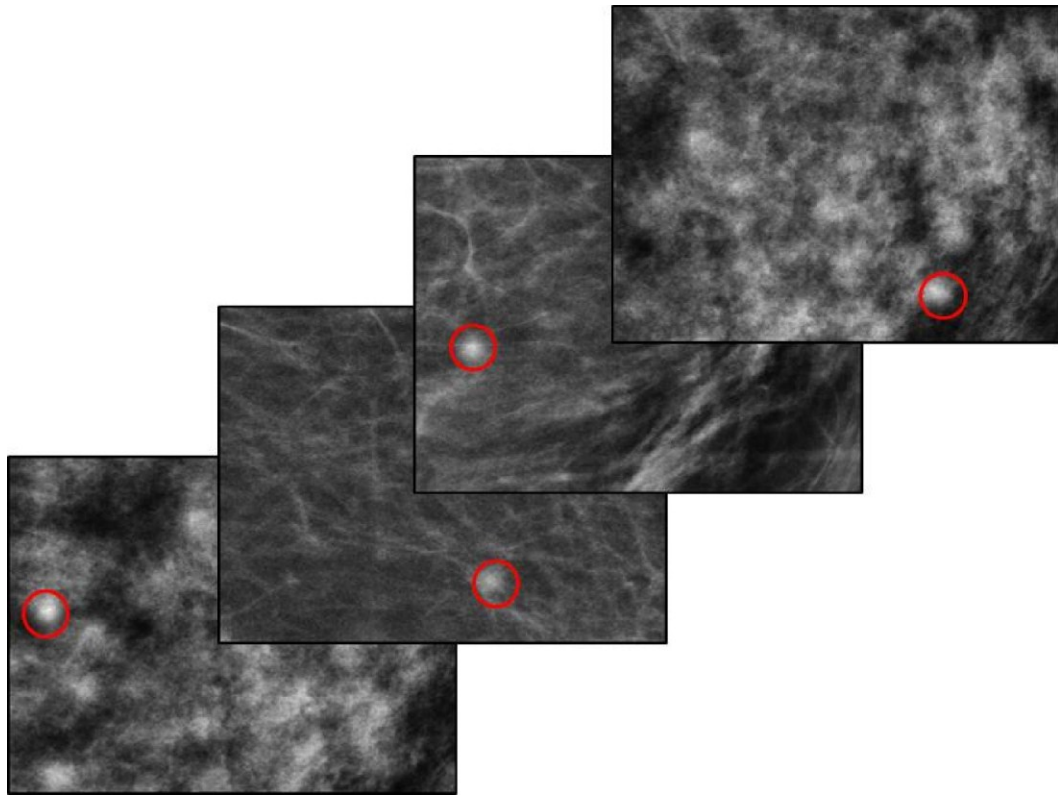
Figure 16. Examples of different test stimuli with varying target contrasts (circled).

followed by the visual search task. In the adapt conditions, the search task was

instead preceded by adaptation for 5 minutes to fatty or dense images. In both

the pre-adapt and adapt conditions there was warning signaled by a tone 5

seconds prior to the presentation of the test stimuli. The adapting stimuli filled the

monitor screen, and cycled randomly through 10 samples at a rate of 250 ms per

image to ensure that participants were adapting to the characteristic texture of

the mammograms rather than to a single image. During the search task, a test

image was randomly selected from either the dense or fatty set, and onset

presentation of the image was accompanied by a tone. Observers used a button

press to respond as quickly as possible whether the target fell on the left or right

side of the monitor screen. A separate button was also available to respond if

they could not find the target. The test image remained on the screen until a response was made. This was then followed by 4 sec readapt period to the gray screen or adapting images, followed by the presentation of the next test image. The program terminated after participants had made 8 repeated settings on each image. To avoid learning the repeated test images or target locations, the test stimuli were shown either in their original orientation, mirrored along the horizontal or vertical axes, or rotated 180 deg (with 2 repetitions of each variant). Results are based on the average settings of the ten subjects, and included all trials in which the target location was identified correctly.

Results

Reaction times varied widely across images. Again this is as expected, since the target contrast was intentionally varied over a wide range to vary the difficulty of the task. To quantify the effect of contrast, for each test we
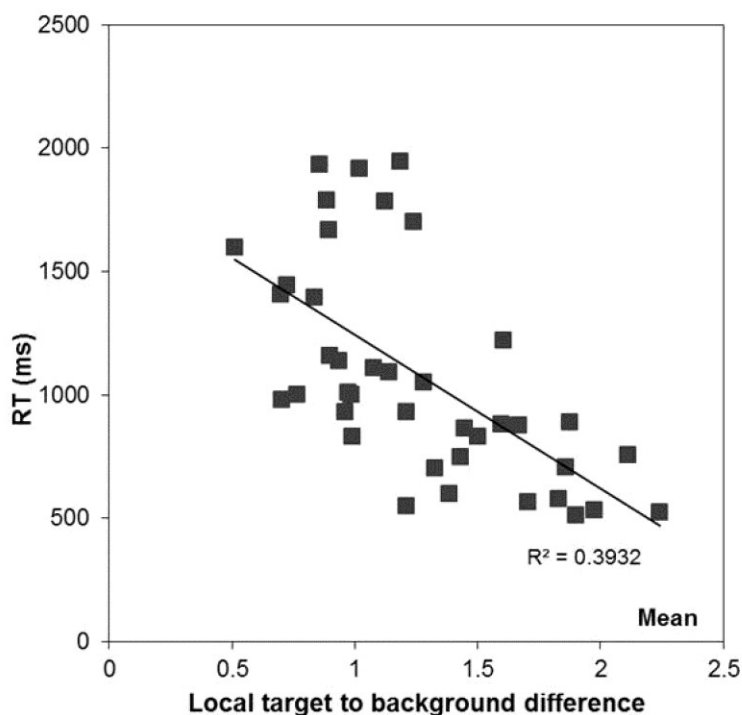

Figure 17. Variation of mean reaction times across images can be partly accounted for by measuring the local contrast by comparing the relative luminance of the target and local surround (r= .63, p < .01).

calculated the local contrast by comparing the relative luminance of the target and the local surround. Figure 17 shows that this measure of local contrast can partly capture the differences in search times across the different images ($r = .63$, $p < .01$).

RT following adaptation to dense images
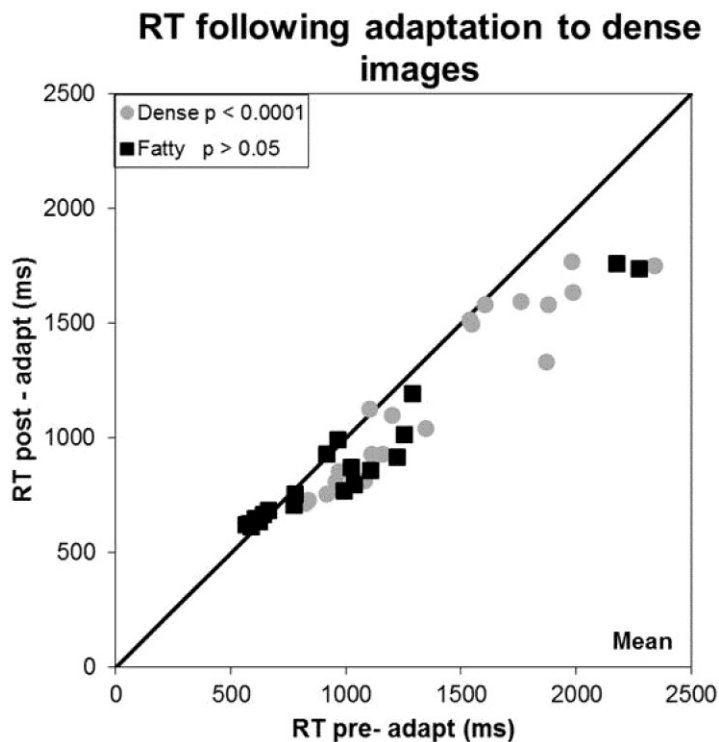
Figure 18. Adaptation to dense images consistently improves detection when searching within dense images, but not fatty, $Z = 3.8$, $p < .0001$.

The remaining figures illustrate the effects of adaptation on the search times. Figure 18 compares the search times before or after adapting to the dense adapting set. Adaptation to the dense images consistently improved detection when searching for targets in dense images (light gray circles), but not fatty (black squares). That is, search times were faster for the same image after adapting than before adapting for the dense images but not the fatty images. This was verified by a sign test comparing the pre- and post-adapt reaction times ($Z = 3.8$, $p < .0001$ for dense; $Z = .22$, $p = .413$ for fatty). Similar effects were also found when analyzing the results only for the 8 naïve observers ($Z = 2.91$, $p = .0013$ for dense; $Z = .92$,

p =.1796 for fatty). Notably, overall accuracy did not differ across the conditions (Figure 19). Thus, the improvements in search times for the dense images did not reflect a speed-accuracy trade-off, suggesting that they instead reflect actual changes in search efficiency.

Figure 20 plots comparable results for the condition where observers instead adapted to the fatty image set. This led to similar results, in that observers' search times were reduced following adaptation for fatty images, but not dense, (Z = 2.91, p =.0013 for fatty; Z = 3.35, p = .0002 for fatty when authors EK and MW were excluded). Again this reduction in reaction time was not due to a speed-accuracy trade-off (Figure 19).
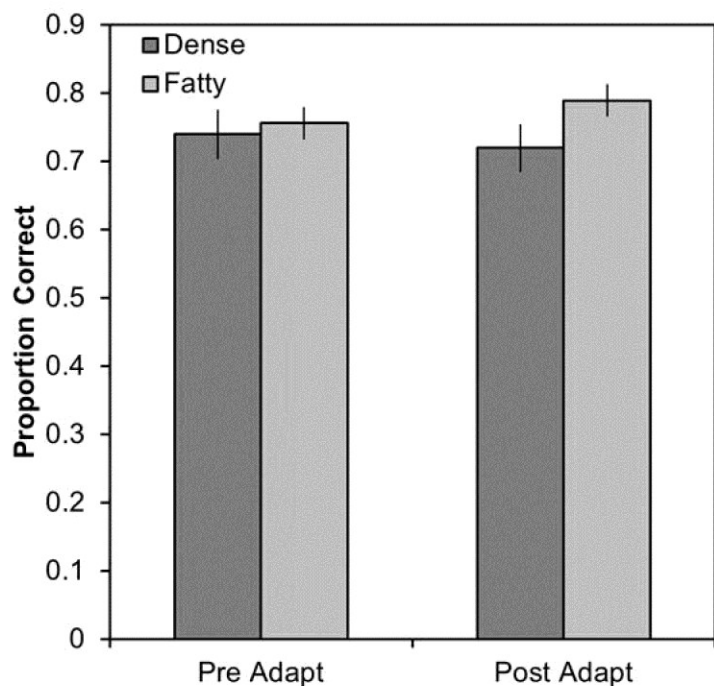
Figure 19. Adaptation to fatty and dense images did not cause a significant change in accuracy compared to the neutral (gray field) adapt.

In both cases the reaction times improved only when the test backgrounds and adapt backgrounds were drawn from the same class of images. Thus the effects of the adaptation were not a general but instead selective for the specific characteristics that distinguish the dense and fatty image. This is based on comparisons of each aftereffect relative to the pre-adapt baseline. However, as a
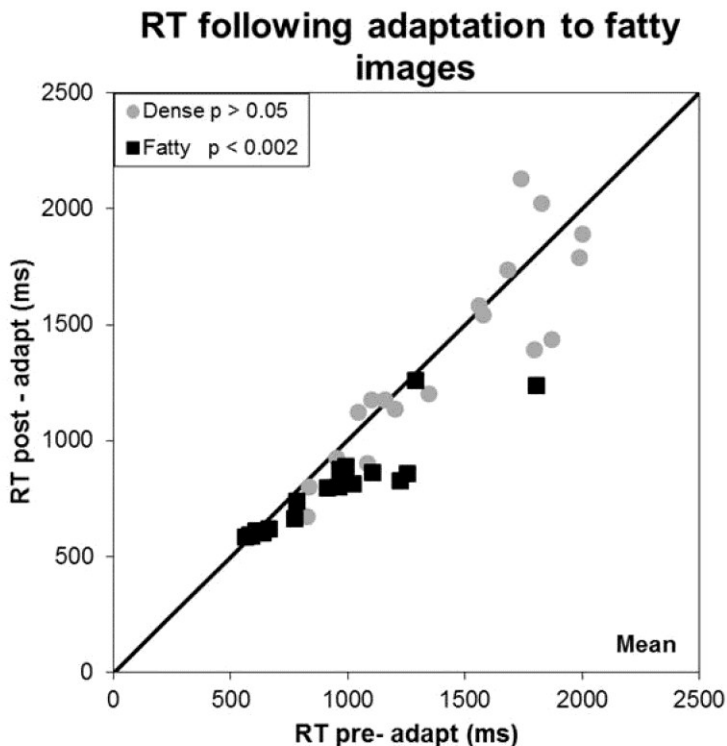
Figure 20. Adaptation to fatty images consistently improves detection when searching within fatty images, but not dense, Z = 2.91, p = .0013.

further test of this selectivity, we also directly compare the search times for the dense or fatty test images when observers were adapted to either the dense or fatty images (Figure 21). Again, this analysis confirmed that adaptation selectively facilitated detection of the simulated tumors when searching on the same image type as the adapt condition, (dense: Z = 3.35, p =.0002; fatty: Z = 2.46, p = .006) (Figure 21).

Discussion

Our results demonstrate that prior exposure to dense or fatty images facilitates search for target "lesions" embedded in mammogram images. Moreover, this enhancement is specific to the adapting image type (dense or fatty) and thus reflects selective performance improvements rather than simple generic learning. This selectivity is consistent with the selectivity we observed previously in the appearance of the mammograms after adaptation (Chapter II).

There we showed that adapting to the dense (or fatty) images causes an intermediate image to appear more fatty (or dense). Thus the adaptation itself must be selective for the textural properties that differentiate the two classes of mammograms.

But why should this selective adaptation impact visual search? As noted in the introduction, one putative role for sensory adaptation is to discount expected properties of the world in order to enhance or draw attention to more novel properties. In fact, we previously also observed aftereffects consistent with this account in the appearance of the images. Specifically, adaptation to the dense or fatty images caused the adapting images themselves to appear less fatty or less dense over time. This suggests that the textural characteristics of the backgrounds became less distinct or more neutral in appearance with prolonged viewing, consistent with a renormalization of perception with adaptation. Similar normalization effects have been observed across multiple stimulus domains, including color (M. A. Webster, 2011a), blur (Elliott et al., 2011), and faces (Rhodes et al., 2005; M. A. Webster & MacLeod, 2011).

If this "desensitization" affects the background more than the target, then a consequence of the adaptation is that it will increase the effective signal to noise ratio of the target, and thus enhance its salience. Again, effects of this kind have been observed previously when adapting to fairly simple stimulus dimensions such as a distribution of colors (McDermott et al., 2010) or arrays of oriented elements (Wissig et al., 2013). They have also been predicted from analyses in which images are processed to simulate the perceptual consequences of very

long-term adaptation to specific environments (M. A. Webster, 2011a). Here we have shown that these effects can potentially also arise over very short timescales within the naturalistic and ecologically relevant task of an individual inspecting a mammogram. The decreased sensitivity to static or ongoing features of the world may draw one's attention to environmental stimuli that differ from the norm, thus highlighting novel properties within the visual scene. At a physiological level, visual performance may be optimized by reducing neuronal firing to the unchanging characteristic properties of the visual scene while increasing the firing rate to novel properties or changes in the environment.

In images with well-defined properties such as distributions of colors or orientations, it is straightforward to define in what ways a target is novel from the background. However, with more complex and naturalistic patterns it
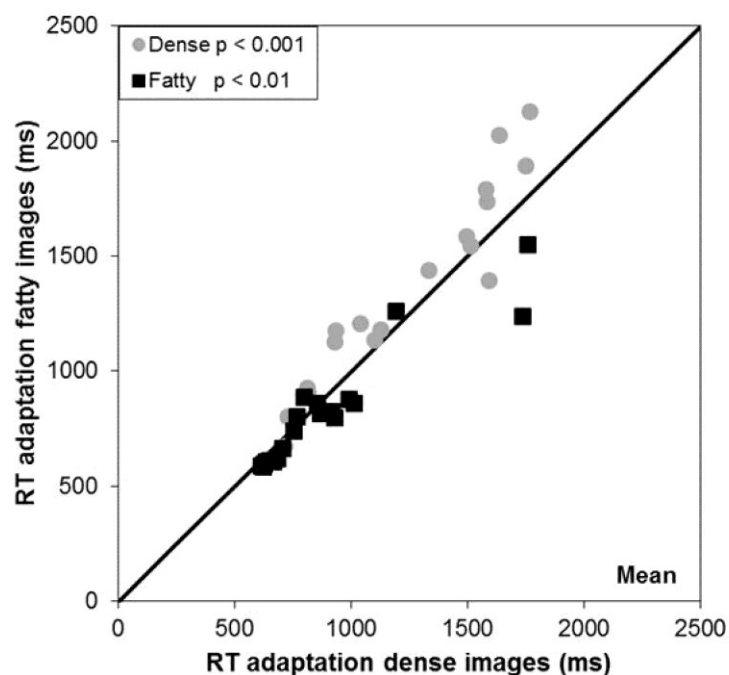

Figure 21. Search within each image type is enhanced after adapting to the same image type, dense: Z = 3.35, p = .0002; fatty: Z = 2.46, p = .006.

less obvious, and in particular, we cannot quantify how the Gaussian target

differs from the dense or fatty background. However, our results are consistent with adaptation acting selectivity on the textural characteristics of the backgrounds relative to the targets.

Our results have a number of practical implications for visual inspection of medical images. Radiologists have very diverse techniques when searching within and classifying mammograms images, and there is relatively little standardization of inspection protocols. Moreover, in general each image is examined n an arbitrary order. The present results suggest that this order could potentially influence their state of adaptation, and thus impact their ability to classify or find information in the images. For instance, if they are looking at a dense scan and then switch to a fatty image, this could bias their classification of the current image under inspection. Moreover, our study suggests depending on which images they have viewed in the immediate past, the radiologist may be in either a better or a less optimized state of adaptation to detect tumors or lesions within the tissue shown in the current image. This suggests that ordering images by their density type could potentially increase search efficiency, which might in turn reduce fatigue. Finally, to the extent that the nature of these adaptation effects and the relevant visual structure of radiological images could be appropriately modeled, it should in principle be possible to develop image processing models to simulate how medical images should appear to observers after they are adapted (in the same way that these models have been developed to simulate the consequences of theoretically optimal color adaptation; (M. A. Webster, 2011a). That is, mammogram images could be "pre-adapted" so that

they are optimized for the visual system of the radiologist, removing the time and effort required for the radiologist to instead adapt to the image.

V. Neural Correlates of texture adaptation and visual search in mammogram images

As noted above, the process of adaptation influenced the judgements of perceived texture as well as performance in a target detection task suggesting adaptation may play a significant role in their interpretation. However, the neural correlates of these adaptation infleunces on image recognition are largely unknown in general and even less is known within the context of medical images. The current study was designed to determine neural correlates of the behviorally measured aftereffects. Using EEG, we were able to explore the timecourse of these visual afterffects and identify neural signatures of these adaptation effects. First, we investigated neural dynamics of classifying mammogram images, based upon their textural properties (fatty vs. dense) and the influence of adaptation upon the neural response. Second, we examined the impact of adaptation upon the neural response between images that contain a simulated tumor vs. normal images (no "tumor"). These studies elucidated when adaptation is occurring during visual processing and its effect on classifcation and target detection when inspecting mammogram images.

Materials and Methods

Observers:

Eight observers with corrected-to-normal acuity participated in the experiments. The observers included author EK and 7 students who were naïve to the purpose of the study. Prior to participation, observers provided written informed consent according to the standards of the university's Institutional Review Board.

Procedure:

1. Neural correlates of texture adaptation in mammograms

All stimuli were presented using the Psychophysics Toolbox (Brainard, 1997) for MATLAB (Mathworks Inc., Natick, MA). The images were displayed on a Mitsubishi Diamond Pro 2070SB monitor (22 inches, 1024 × 768) with a refresh rate of 85 Hz. Behavioral responses were recorded via a keyboard press. Stimuli consisted of randomly selected sections taken from a database of normal mammograms (Chen et al., 2012) previously classified with a BI-RADS Density score of fatty or dense. The sections consisted of 256 × 256 pixel sections in the original 2560 by 3328 images and were constrained to be fully within the breast region of the image. The 8-bit pixel values were rescaled so that the average luminance (37 cd/m^2) and rms contrast (.38) were constant across all images. 155 images from each category (dense and fatty) were used resulting in 310 total images. Observers initially adapted for 60 seconds (s) to a dynamic array of either dense or fatty images, each randomly displayed for 250 ms, in order to avoid local light adaptation. The adapting sequence and test images were

separated by a 2 s uniform gray screen (19 cd/m^2) and subsequent test stimuli

were interleaved with 4-6 s random periods of readaptation. The test images

were each randomly displayed for 30 ms, and the participant indicated via a

button-press whether the image was dense or fatty. Between each test image, a

blank gray screen containing only a fixation point was presented for a random

inter-trial interval of 600-900 ms. The trial sequence is shown in Figure 22.
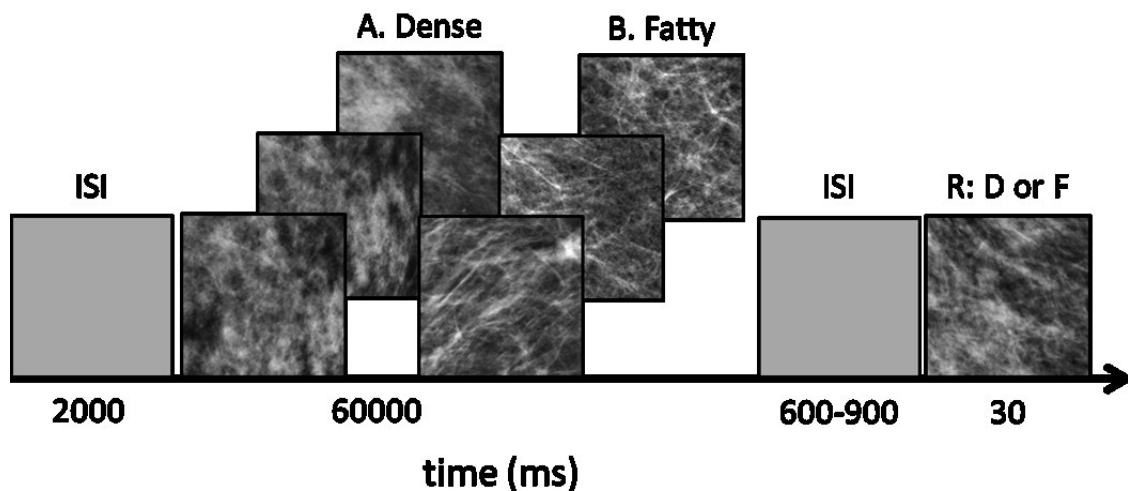
Figure 22. Stimuli and trial sequence. ISI represents the interstimulus interval between the adapting array and test stimuli. Observers either adapted to A. a dynamic dense array or B. a dynamic fatty array of images and then were tasked with signaling with a button press if the test image was dense (D) or fatty (F).

2. Neural correlates of adaptation and target detection in mammograms

Participants completed a behavioral task where observers responded with

a button-press if there was a target present or absent in the image, while EEG

was recorded. The stimuli consisted of randomly selected sections, identical to

the procedure described above. There was a total of 300 images with an equal

number of dense images without targets and dense images with simulated

tumors added randomly within the tissue. Simulated lesions were created using

Gaussian spots (SD = .18º), superimposed at random locations in the test stimuli

by adding luminance to the background. Target contrast varied over 5 levels so

that detection varied from easy to difficult. All other methods were identical to

those listed above.

Following the initial test examining the average waveform difference

following adaptation when searching for "tumors" embedded in dense tissue, we

investigated how adaptation to dense or fatty images would influence search

within both dense and fatty scans. The task was the same as described in 1

(Figure 22), except that participants instead indicated target presence or absence

in dense and fatty images (150 dense and 150 fatty). Additionally, there were 5%

catch trials in which the observer responded to target absence and these were

randomly displayed amongst the images with targets.

EEG data acquisition

Continuous EEG was recorded using NetStation 4.5.1 from a 256-channel

HydroCel Geodesic Sensor Net (Figure 23) via a Net Amps 300 amplifier

(Electrical Geodesics Inc., Eugene, OR) at a sampling rate of 1000 Hz. Onset

event-related potentials (ERP's) were recorded at each electrode site and EEG

epochs were time locked to stimulus onset beginning 100 ms prior to the start of

each test image and continuing until 800 ms following the stimulus presentation.

These recordings were taken from the continuous recording stream and the

artifact-free sections were averaged across subject based upon their image

category (dense or fatty, target presence or absence). All 256 channels of

continuous EEG were first order high-pass filtered at 0.3 Hz and then low-pass filtered at 30 Hz using a finite impulse response (FIR) filter. For all experiments, the continuous EEG was segmented by trial type (adapt dense or fatty or target) and time locked to the onset of each image. The first 500ms was discarded to exclude the visual evoked potential (VEP) to flicker onset in the estimation of averaged amplitudes. Artifact rejection routines were applied to the segmented EEG data to identify segments containing common artifacts. Channels were identified as containing artifacts if the segment contained amplitude values exceeding 200 µV (microvolts). Additionally, segments containing eye blinks with amplitude values greater than 140 µV were rejected prior to further analysis. Finally, segments containing eye movements with amplitude values greater than 55 µV were discarded.

After artifact detection routines were applied to the segmented EEG, data from bad channels were interpolated from surrounding electrode sites. For all experiments, data segments from each trial were then averaged separately for each participant. The averaged data was then re-referenced to the average reference channel (Cz). Finally, baseline correction was performed on the averaged, re-referenced data using the 100 milliseconds prior to stimulus onset as the defined baseline period.

Analysis:

Performance was evaluated based upon accuracy and response speed (reaction time, RT), for each subject and task condition (dense or fatty, target present or

absent). Only correct trials were included in the analysis excluding all incorrect

responses. To assess differences between the obtained ERP curves for the
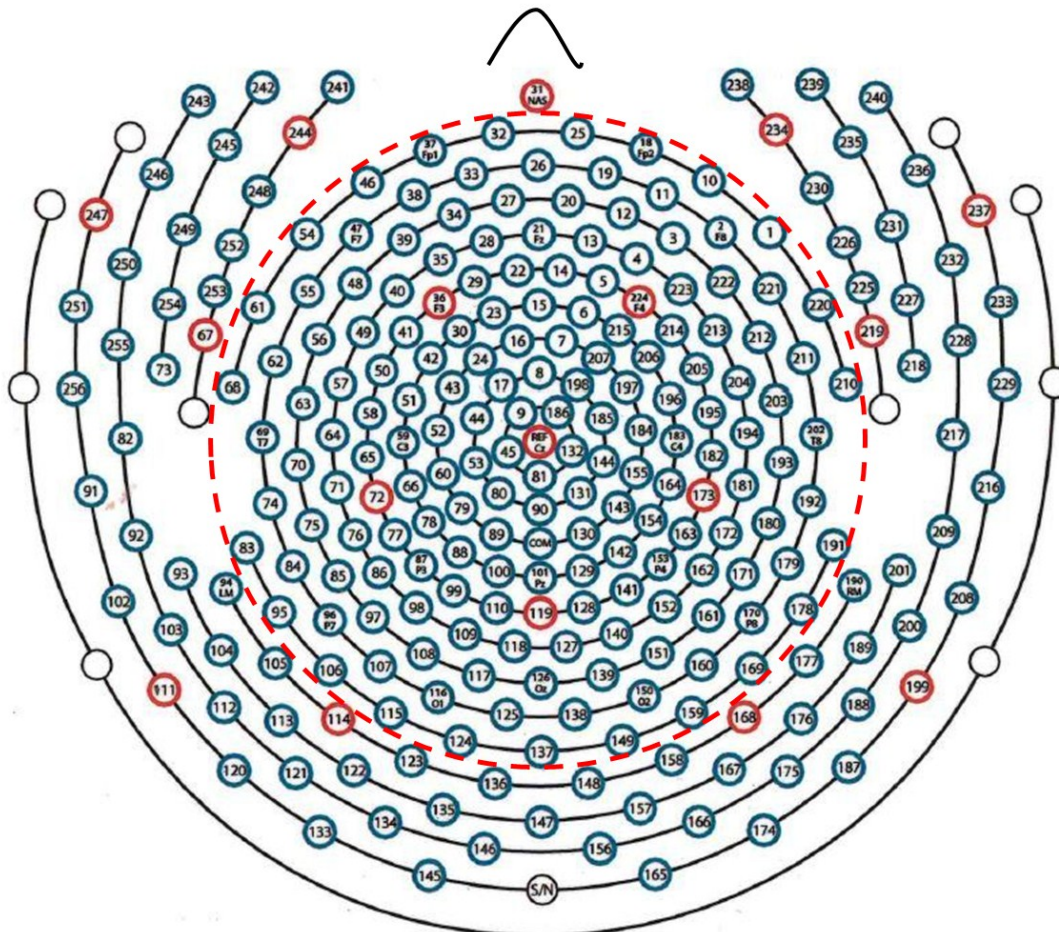
Figure 23. Hydrocel Geodesic Sensor Net, dotted red circle designates scalp electrodes
of interest, electrodes that fall outside the circumference of the circle include areas
covering the neck and face.

 dense trials vs. the fatty trials (target presence vs. absent trials) we used

a similar method to Rugg et al. (Rugg, Doyle, & Wells, 1995). To investigate if

there was a differential effect present between the two waveforms, a criterion of

at least 15 consecutive significant t-values in the 1000 Hz time sample was

applied when performing a point-by-point comparison on the subtraction

waveforms between the trial conditions. This analysis was performed at specific electrode sites of interest (Oz, O1, O2, Pz, P4, P3, P7 and Fz). In addition, a topographic analysis was conducted to investigate the influence of adaptation on distribution of activity across the scalp. The benefit of this analysis is that rather than restricting the data manipulation to single electrode sites (as in the study by Rugg et al.), changes in the activity can be observed across the entire scalp at all time points during the trial duration.

The statistical analyses for topographical maps were conducted offline in MATLAB. Paired sample t-tests were conducted on every electrode and time point during the trial (1000 Hz) duration at each electrode per condition (dense vs. fatty, or target present vs. absent). We were specifically interested in examining how the adapt condition (dense or fatty) would influence the overall pattern of activity across the scalp distribution while viewing the same or different image types. In addition, we examined effects of adaptation on target present and target absent images for both image categories. P-values obtained from the t-tests were thresholded at $p < .05$ for each electrode and time point and imported back into NetStation to visualize significant differences in activity between conditions. Using this method, we were able to determine specific time windows of interest to be used for further analysis. This manipulation allowed us to isolate waveform components of interest across various regions of the scalp (frontal, parietal, occipital and temporal).

Results

1. Neural correlates of texture adaptation in mammograms

Behavioral Effects

We were interested in further elucidating how adaptation to dense or fatty images influenced subsequent classification of dense or fatty images. We hypothesized that adaptation to fatty (dense) images would result in more efficient categorization of fatty (dense) scans. We conducted a sign test comparing reaction times post-adaptation to dense and fatty scans when categorizing the textural properties of the images. There was no

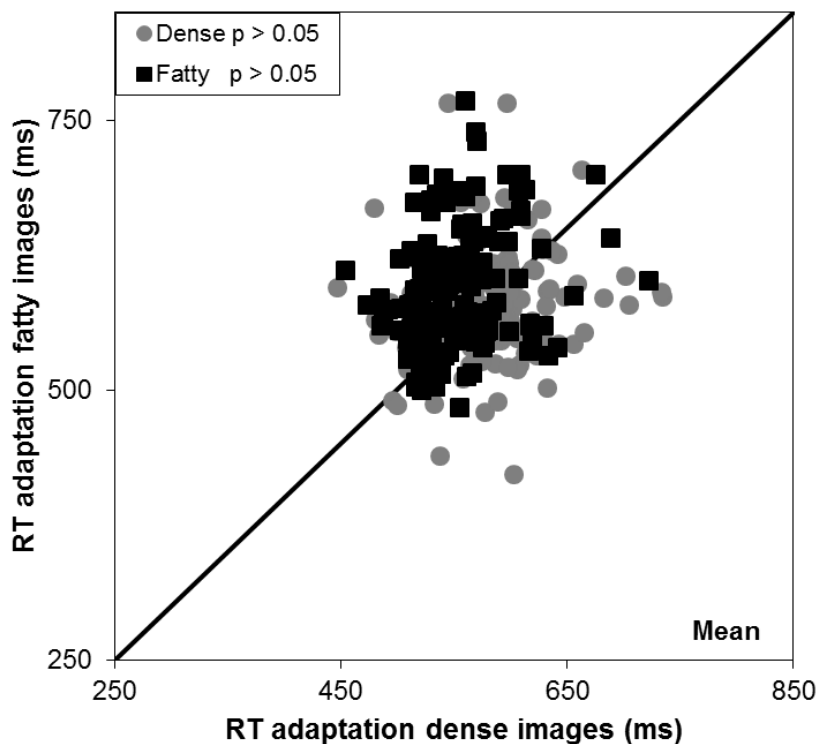**Figure 24.** Adaptation to dense and fatty images does not consistently improve classification of subsequent fatty (plotted black squares) or dense scans (plotted gray circles). (fatty images: Z = -5.94, p = .9999; dense images: z = 1.29, p =.0993.)

significant effect of adaptation (Figure 24, fatty images: Z = -5.94, p = .999; dense images: Z = 1.29, p =.099). This suggests that when given only a short

duration to view the images (30 ms), adaptation to the different textural

properties does not influence how quickly subsequent images are classified.

EEG Results

   Concurrently, we were interested in how adaptation to the textural

properties of the mammogram scans would alter the difference waveforms when

categorizing fatty or dense scans. As discussed in the analysis section above, we

subjectively evaluated significant timepoints of interest between the adapt

conditions (fatty or dense). We then quantified the mean of the significant

electrodes for timepoints of interest to create an average waveform for the

different significant components. As can be seen in Figure 25 (top), there was no

significant difference between adapt condition when categorizing fatty images at

occipital or frontal sites during any timepoints of interest following post-stimulus

onset (Figure 25., top, panel a: average t = -.3910, average p = .6069, df = 8;

panel b: average t = .2185, average p = .6741, df = 8; panel c: average t =

1.7241, average p = .1796, df = 8). Plotted in the lower panels are the difference

waveforms between the adapt conditions, clearly revealing non-significant

differences. Topographic activations during the timepoints of interest reveal

similar non-significant patterns between the adapt conditions (Figure 25, bottom

row). Moreover, we see similar patterns when observers instead categorized

dense images, Figure 26, top (panel a: average t = .7066, average p = .5301, df

= 8; panel b: average t = -1.4974, average p = .2304, df = 8; panel c: average t =

.5169, average p = .6290, df = 8). This mirrors the behavioral results in that

Fatty Images

Figure 25. There were no significant effects of adaptation on subsequent categorization of fatty images. Average waveforms for electrode sites of interest, labeled in upper left corner of panels a. – c., for trial duration. Top panels plot the average waveforms when categorizing fatty images and lower panels plot the difference waveform between the two conditions. Red lines depict the average waveform following adaptation to fatty scans and blue lines show the average waveform following adaptation to dense images. Topographic activations during the timepoints of interest (listed next to the topographic maps) are plotted at the bottom displaying the differential activations, corresponding to the difference waveforms (plotted in green). (Fatty Images: panel a: average t = -.3910, average p = .6069, df = 8; panel b: average t = .2185, average p = .6741, df = 8; panel c: average t = 1.7241, average p = .1796, df = 8).
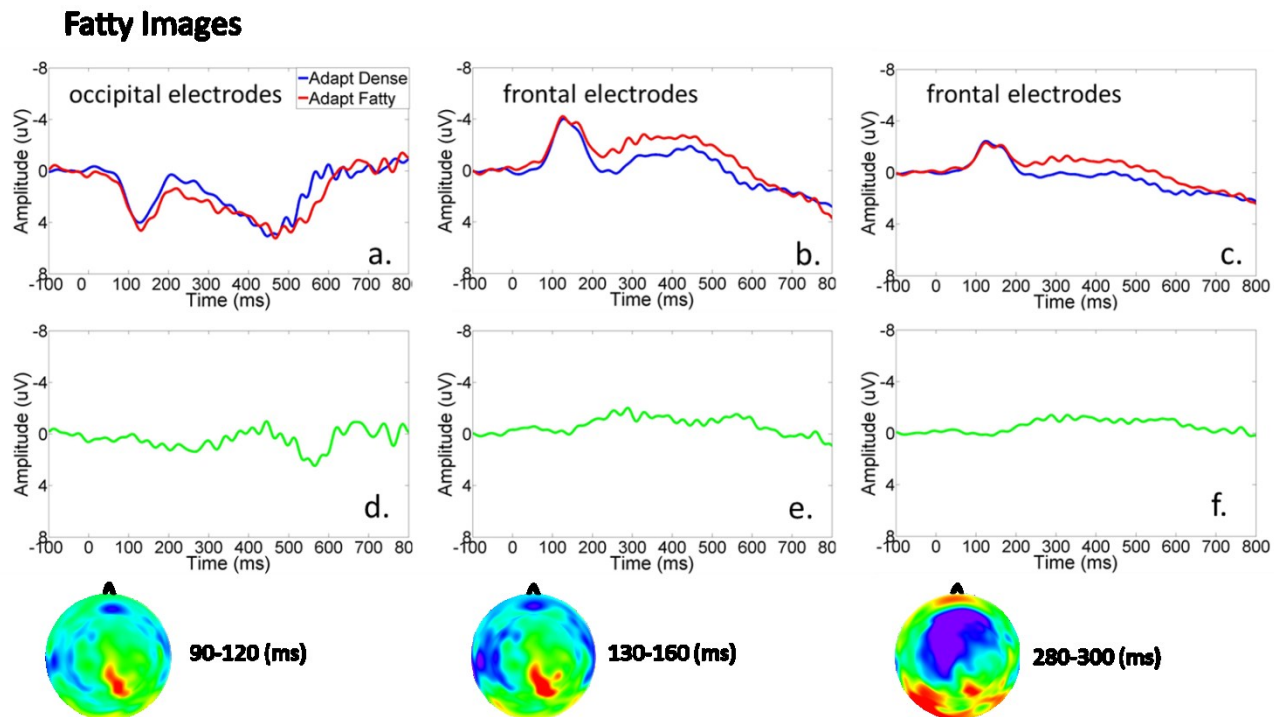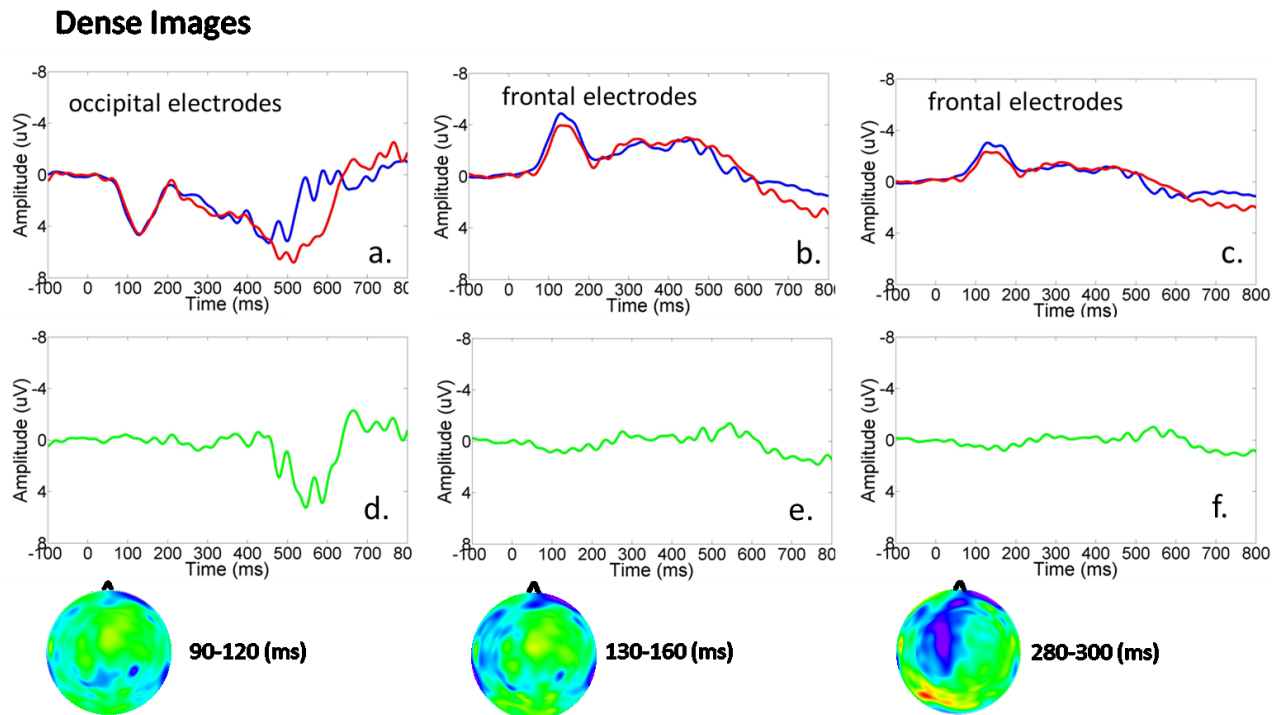
Figure 26. There were no significant effects of adaptation on subsequent categorization of dense images. Average waveforms for electrode sites of interest, labeled in upper left corner of panels a. – c., for trial duration. Top panels plot the average waveforms when categorizing dense images and lower panels plot the difference waveform between the two conditions. Red lines depict the average waveform following adaptation to fatty scans and blue lines show the average waveform following adaptation to dense images. Topographic activations during the timepoints of interest (listed next to the topographic maps) are plotted at the bottom displaying the differential activations, corresponding to the difference waveforms (plotted in green). (Dense images: panel a: average t = .7066, average p = .5301, df = 8; panel b: average t = -1.4974, average p = .2304, df = 8; panel c: average t = .5169, average p = .6290, df = 8).

adaptation did not cause significant differences between the two waveforms when categorizing fatty or dense images (Figure 25 and 26).

2. Neural correlates of adaptation and target detection in mammograms

Behavioral Effects

Initially, we aimed at investigating the effect of adaptation on target detection when searching within dense scans. We were interested in how adaptation to dense images would influence reaction times when inspecting images for simulated tumors. We hypothesized that adaptation to dense scans would result in more efficient search. We conducted a sign test comparing reaction times for images' containing targets and those without targets both prior to

RT Searching for Targets Pre vs. Post Adaptation

- Target p < 0.0001
- No Target p < 0.0001
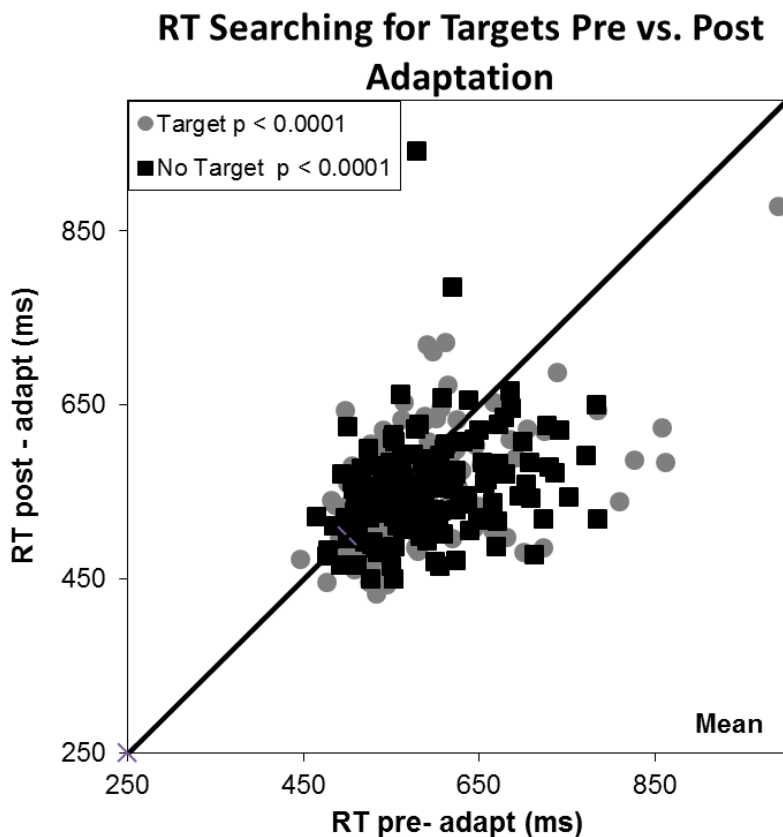
RT post - adapt (ms)

RT pre- adapt (ms)

Mean

Figure 27. Adaptation to dense images consistently improves search efficiency for simulated lesions (plotted gray circles) within scans and correct rejection of images not containing targets (plotted black squares). (targets: Z = 4.55, p < .0001; no targets: z = 4.65, p < .0001.)

and following adaptation. There was a significant effect of adaptation (targets: Z = 4.55, p < .0001; no targets: Z = 4.65, p < .0001) (Figure 27). This suggests that adaptation facilitates more efficient search for simulated lesions such that observers were faster to identify lesions or correctly reject scans lacking "tumors".

EEG Results

Simultaneously we explored the effect of adaptation on the activity of the topographic distribution. As described above, we examined regions of interest (i.e., frontal and occipital recording sites) during significant timepoints. Thus, in our first comparison we examined the difference in waveforms between the target present and target absent trials prior to adaptation (Figure 28). There was no significant difference between the average waveforms (Figure 28, top, panel a: average t = -.3448, average p = .7431, df = 6; panel b: average t = .4668, average p = .6521, df = 6).

Importantly, we were interested in how adaptation would characteristically alter the target and non-target waveforms (Figure 29). As shown in Figure 28, prior to adaptation there was little to no significant difference between target present and target absent trials. However, this was not the case following adaptation (Figure 29, top, panel b). Average waveforms began to diverge approximately 370 ms post-stimulus onset, with greater activation in the frontal electrode sites for target trials compared to target absent images (Figure 29, top (panel a: average t = -.3442, average p = .7429, df = 6; panel b: average t =

Pre Adapt
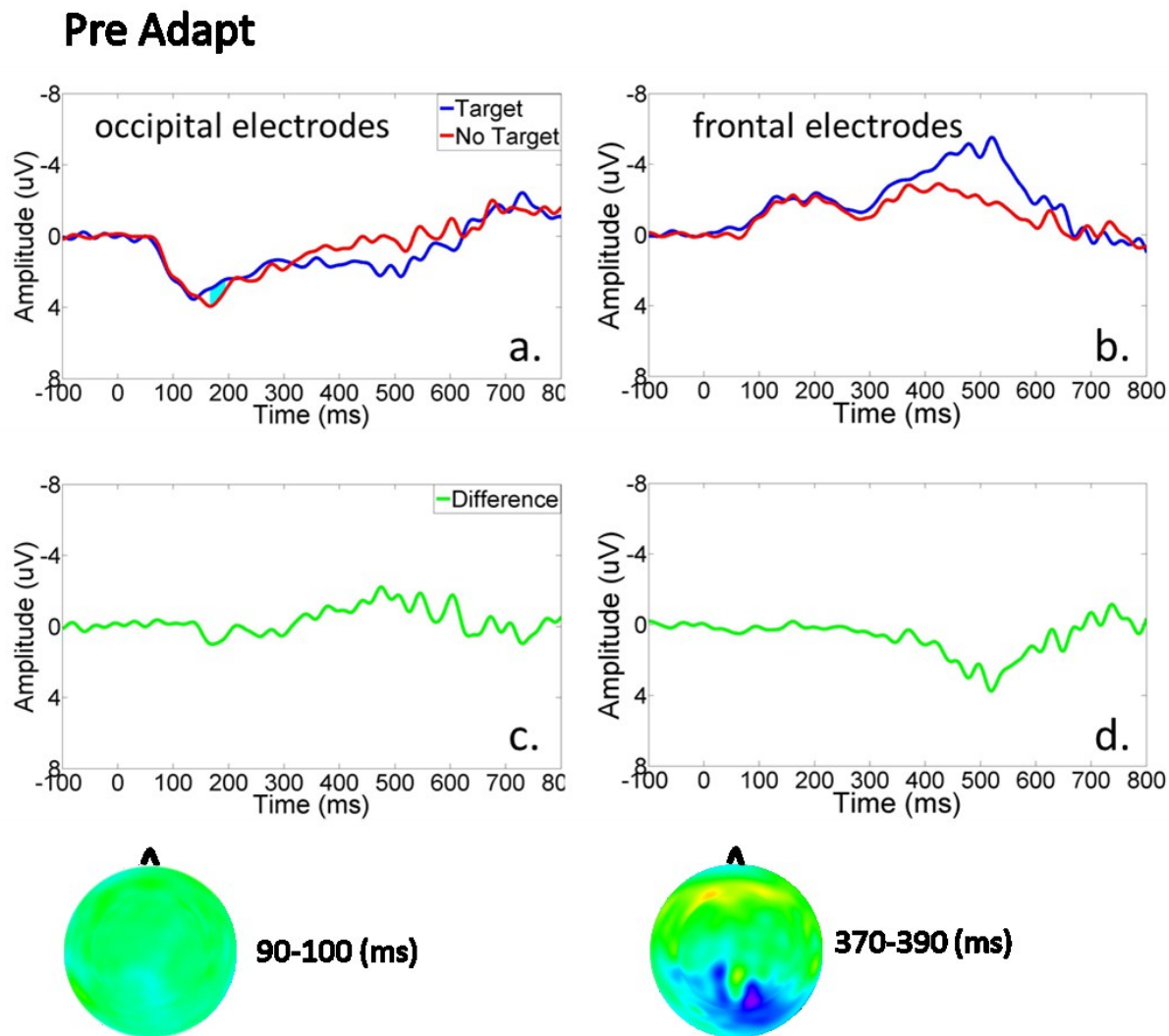
Figure 28. There was no significant difference between images containing target and those without targets prior to adaptation. Average waveforms for electrode sites of interest, labeled in top panels a. – b., for trial duration. Top panels plot the average waveforms when searching for targets in dense images prior to adaptation and lower panels plot the difference waveform between the two conditions. Red lines depict the average waveform for images containing simulated tumors, blue lines show the average waveform for scans without targets and green lines plot the difference waveform between these two conditions. Topographic activations during the timepoints of interest (listed next to the topographic maps) are plotted in the bottom row displaying the differential activations, corresponding to the difference waveforms (plotted in green). Pre- adapt: panel a: average t = -.3448, average p = .7431, df = 6; panel b: average t = .4668, average p = .6521, df = 6).

Post Adapt
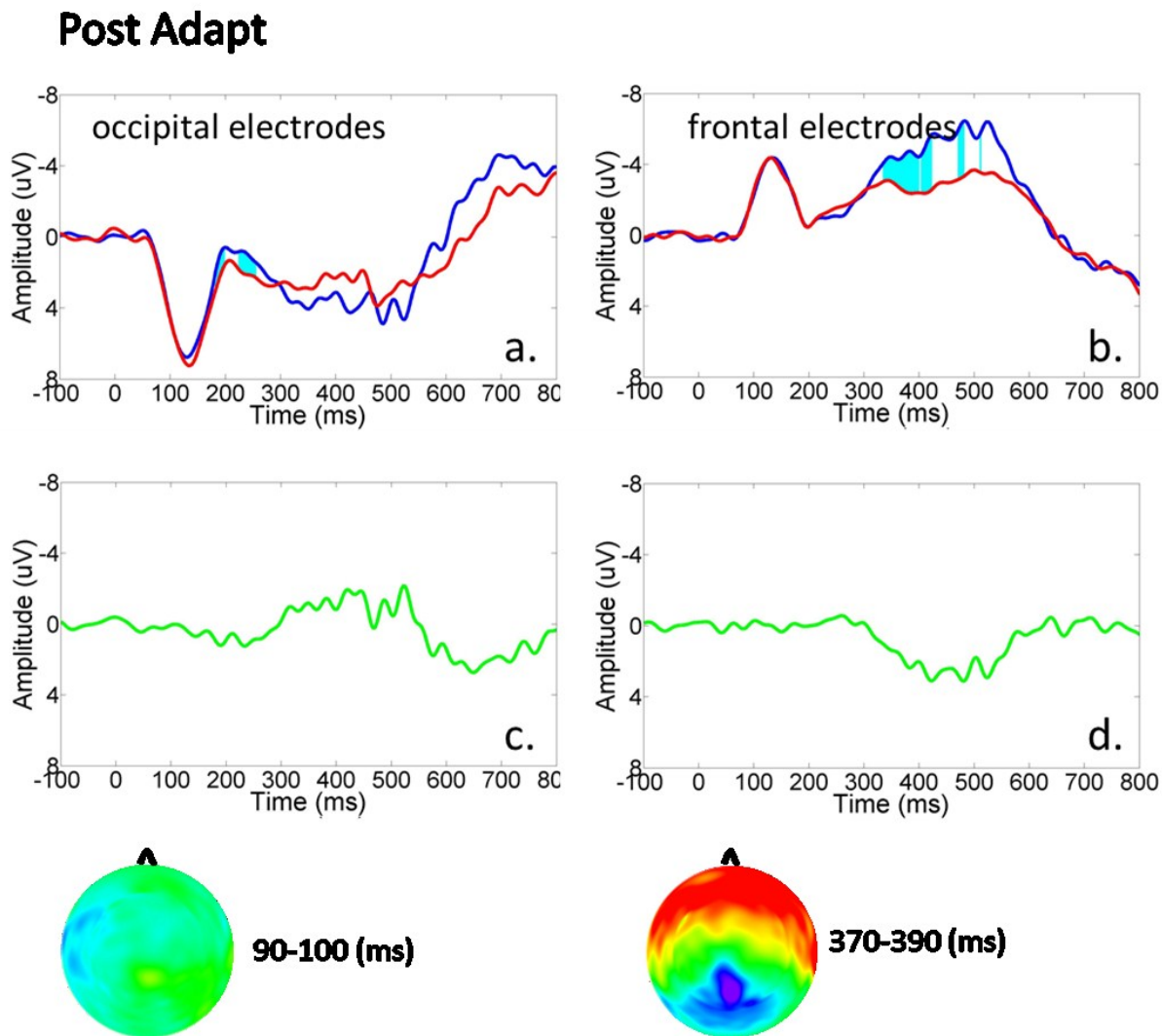
Figure 29. Following adaptation there was a significant difference between target present vs target absent trials, particularly at later timepoints in frontal regions, panel b. Average waveforms for electrode sites of interest, labeled in top panels a. – b., for trial duration. Top panels plot the average waveforms when searching for targets in dense images postadaptation and lower panels plot the difference waveform between the two conditions. Red lines depict the average waveform for images containing simulated tumors, blue lines show the average waveform for scans without targets and green lines plot the difference waveform between these two conditions. Topographic activations during the timepoints of interest (listed next to the topographic maps) are plotted in the bottom row displaying the differential activations, corresponding to the difference waveforms (plotted in green). (panel a: average t = -.3442, average p = .7429, df = 6; panel b: average t = 5.8202, average p = .0020, df = 6).

5.8202, average p = .0020, df = 6). This suggests that adaptation increased later

frontal activity when searching for simulated tumors within medical scans.

Finally, we investigated how adapt condition (dense or fatty) would

influence search on subsequent dense or fatty images. This experiment closely

mirrored the behavioral search study discussed in Chapter IV. We hypothesized

that adaptation to fatty (dense) scans would decrease reaction time and increase

neural activation when searching in the fatty (dense) images. We conducted a sign test comparing reaction times for dense and fatty images' containing targets following adaptation to either an array of dense or fatty images. There was a significant effect of

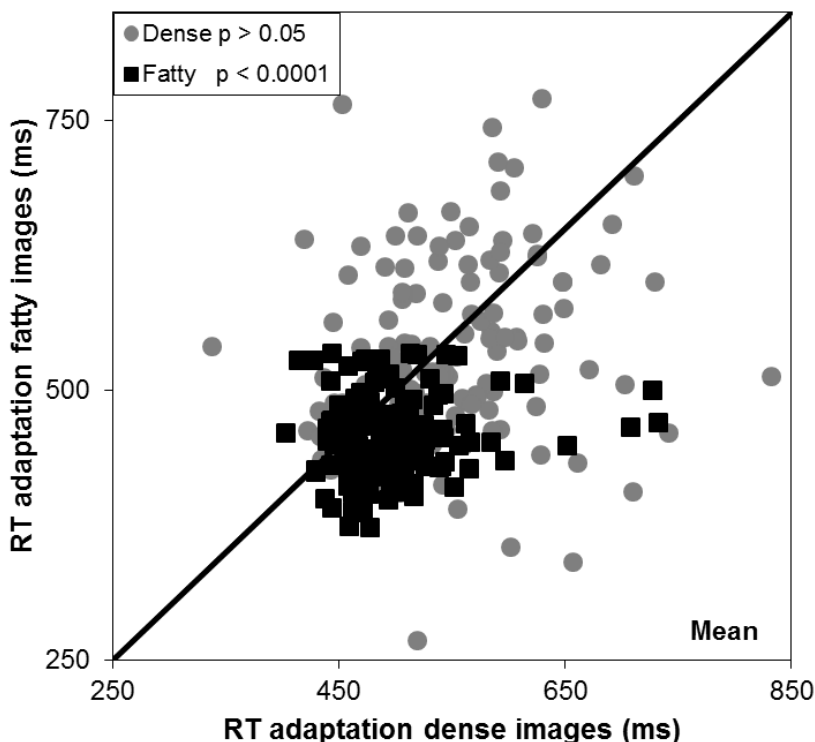**Figure 30.** Search within fatty images is enhanced after adapting to the same image type, fatty: Z = 6.45, p < .0001; however, search efficiency in dense images is not affected by adapting to the same image type, dense: Z = -2.19, p = .9909.

adaptation for fatty images, but not dense (fatty: Z = 6.45, p < .0001; dense: Z =

-2.19, p = .9909) (Figure 30). This suggests that adaptation to fatty

images significantly facilitates more efficient search on subsequent fatty images.

EEG Results

In order to characterize how this manifests neurally we performed a similar topographic analysis as above. Importantly, the manipulation of interest was adapt condition (fatty or dense). We compared the average waveforms for fatty trials following adaption to fatty and dense images (Figure 31). We did an identical comparison for dense scans (Figure 32). For fatty trials there was a significant effect of adaptation to the fatty array relative to the dense during early and late occipital electrode sites (Figure 31, top, panel a-b). (Figure 31, top (panel a: average t = -3.4179, average p = .0223, df = 6; panel b: average t =-2.9979, average p = .0323, df = 6). However, there was not a significant influence of adaptation to dense scans when then searching upon subsequent dense images (Figure 32, top, panel a-b). (Figure 32, top (panel a: average t = -1.2568, average p = .3560, df = 6; panel b: average t =-1.2888, average p = .2768, df = 6).

Discussion

Our results demonstrate that adaptation to the properties of mammograms can significantly alter not only response times, but also modulate neural activity. Previous ERP studies have demonstrated that adaptation occurs at multiple stages and areas in the visual cortex recruiting both feedforward and feedback mechanisms (Niedeggen & Wist, 1998). Specifically, atteuation of the response in early cortical areas is indicative of adaptation to the low level properties of the

adapting stimulus. Where adaptation to more complex stimuli such as faces is relfected at later latencies in the ERP (Kovács et al., 2006). Moreover, adaptation has generally been characterized by an attenuation of the neural response, such that adaptation functions to decrease neuronal resources devoted to unchanging stimuli, thus facilitating the detection and processing of novel stimuli (Kloth & Schweinberger, 2010; Schweinberger et al., 2007). Behavioral research has shown that adaptation to the surface properties of images is at least partially resolved at early areas in the visual processing stream (e.g. LGN and V1; (Motoyoshi et al., 2007). More recent work has implicated separate, parallel pathways involved in the perception of form and texture (Cant & Goodale, 2007; Cant, Large, McCail, & Goodale, 2008). These different properties activate distinct areas of the occipito-temporal cortex, with texture differentially activating the collateral sulcus (CoS), while form information is projected to the lateral occiptial area (LOC) (Cant, Arnott, & Goodale, 2009). Taken together these results suggest that texture adaptation is resolved at multiple levels in the visual processing stream and is an essential property used to recognize scenes and objects.

Radiologists classify mammogram images based upon their textural properties using the BI-RADS Desnity classification system to categorize the breast tissue on a scale from fatty to dense ((ACR), 1998). These tissue classifications are characterized by distinct differences in the appearance of their textural properties, with fatty tissue being striated in appearance and dense tissue cloudier in nature. Due to our previous findings showing robust adaptation

to these textural propeties, fatty and dense, and other work on texture adaptation we hypothesized that prolonged viewing of the images would result in an attentuation of the neural response in occipital areas. Moreover, we predicted a similar pattern in the target detection task except that we postulated an increase in the magnitude of activation in frontal regions in the later waveform components.

Adaptation to the textural properties of mammogram images did not significantly alter subsequent categorization of fatty or dense scans (Figure 24). This contradicts our previous findings revealing that adaptation to dense images resulted in all images appearing more fatty and vice versa (Chapter II). Importantly, these studies did not measure response time to categorize the images. Due to the fact that we did not see a measureable effect of adaptation it is difficult to say if our paradigm was efficient in producing these previously observed effects. Moreover, in the present experiment reaction time may not have been a sensitive measure when investigating the influence of adaptation on the categorization task. Further evidence that adaptation did not significantly affect categorization of subsequent images is shown by the topographical analysis (Figure 25 and 26). Similar to the behavioral findings adaptation to the same image type as classification did not significantly alter the component waveforms of interest.

Fatty images with target embedded

Figure 31. There was a significant increase in the scalp distributions activity following adaptation to fatty images when searching on the same image type (Figure 31, top, panels a-b). Average waveforms for electrode sites of interest, labeled in top panels a. – b., for trial duration. Top panels plot the average waveforms for fatty trials. Red lines depict the average waveform for trials after adapting to a fatty array, blue lines instead show the average waveform for trials following adaptation to dense scans and green lines plot the difference waveform between these two conditions. Topographic activations during the timepoints of interest (listed next to the topographic maps) are plotted in the bottom row displaying the differential activations, corresponding to the difference waveforms (plotted in green). (fatty: panel a: average t = -3.4179, average p = .0223, df = 6; panel b: average t = -2.9979, average p = .0322, df = 6)
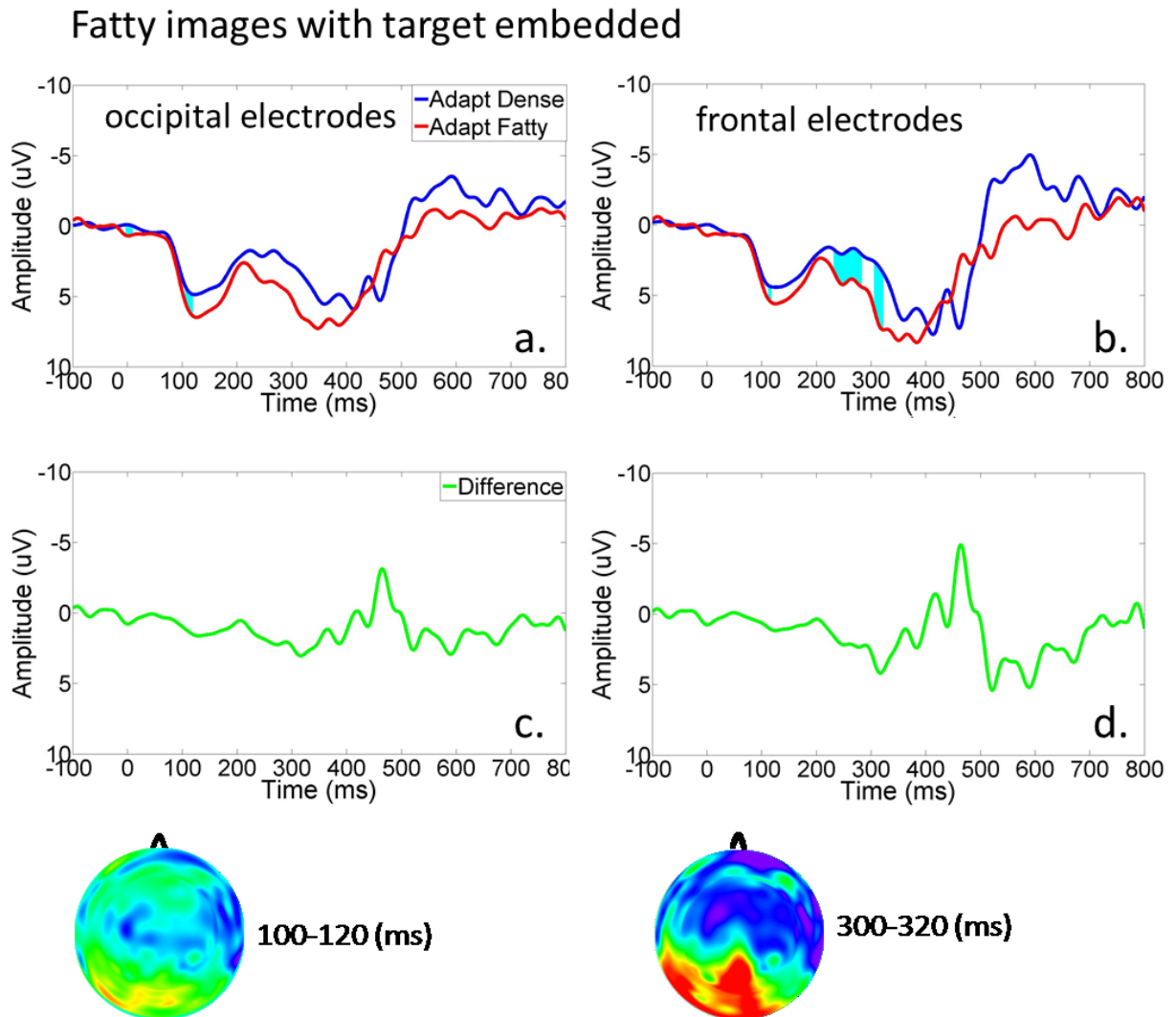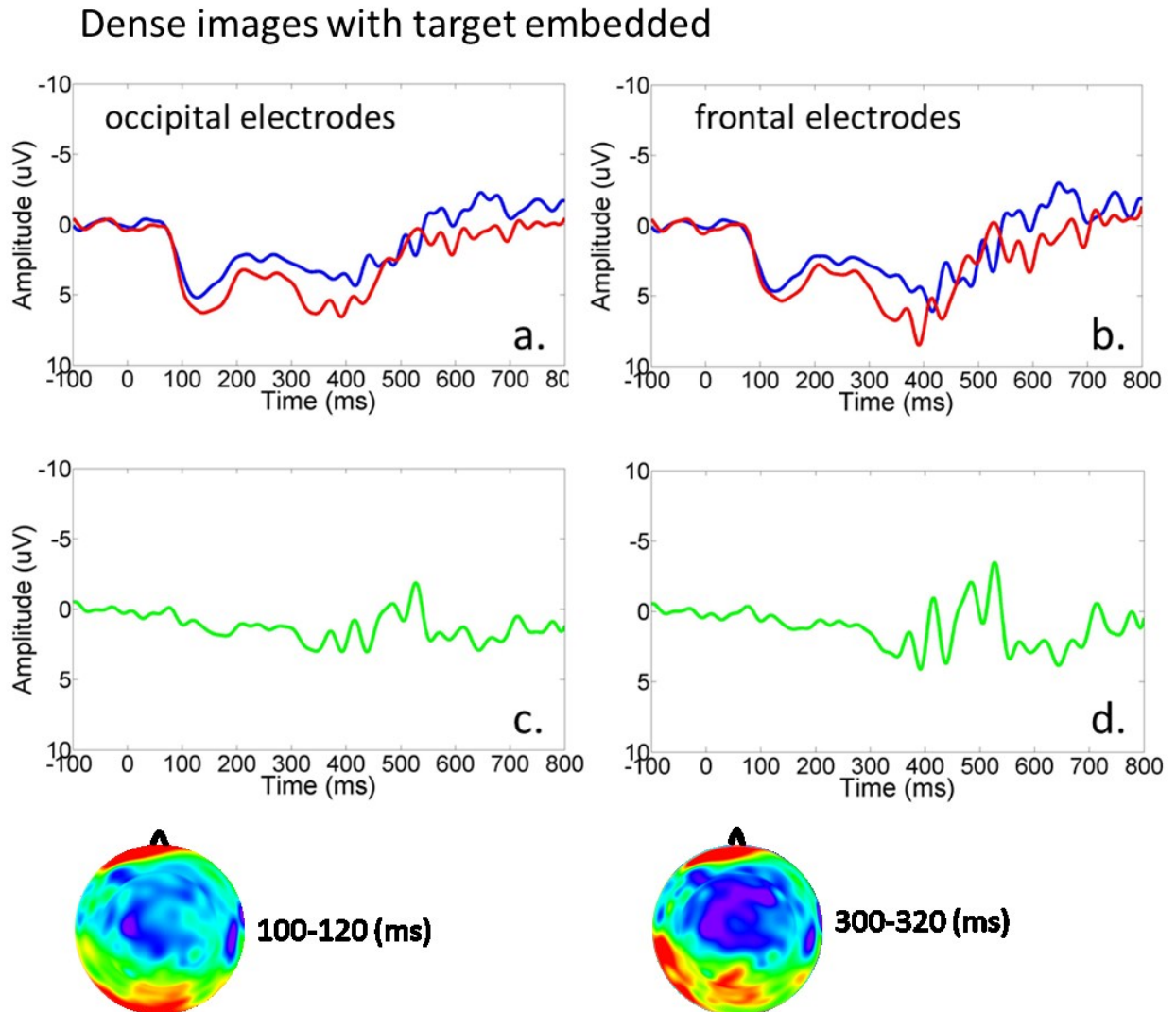
Figure 32. There was not a significant increase in the scalp distributions activity following adaptation to dense images when searching on the same image type (Figure 32, top, panels a-b). Average waveforms for electrode sites of interest, labeled in top panels a. – b., for trial duration. Top panels plot the average waveforms for dense trials. Red lines depict the average waveform for trials after adapting to a fatty array, blue lines instead show the average waveform for trials following adaptation to dense scans and green lines plot the difference waveform between these two conditions. Topographic activations during the timepoints of interest (listed next to the topographic maps) are plotted in the bottom row displaying the differential activations, corresponding to the difference waveforms (plotted in green). (dense: panel c: average t = -1.2568, average p = .3560, df = 6; panel d: average t = -1.2888, average p = .2768, df = 6)

In contrast, viewing the radiological scans facilitated search efficiency when signaling target presence and absence (Figure 27). Our present findings suggest adaptation modulates the late onset divergence in target present vs. absent waveforms in frontal regions at approximately 370 ms. This modulation is characterized by a significant increase in the distribution of scalp activity suggesting greater neuronal contributions devoted to target detection. Specifically, observers were able to more quickly decide if the images contained an abnormality (target) or not. We propose that target detection involves a form of the P300 component reflected by the late divergence in the waveforms present at 370 ms post-stimulus onset (Figure 29, panel b). Previous studies have shown similar findings, in which target presence was accompanied by an increase in the amplitude of P300 component relative to stimuli without targets (Hope et al., 2013). Interestingly, this was one of the only studies to explore the electrophysiological correlates of target detection in medical images. It is important to note we were interested in the effect of adaptation on the neural response, whereas the former experiment addressed modulations of the ERP waveform dependent upon target presence or absence. Contrary to their results we did not observe a significant increase in the P300 component based solely on the introduction of a "tumor" into the image. This could possibly be attributed to paradigm and stimuli differences. Specifically, the simulated lesions that were introduced into their images were large is size and added to the images directly in the center of the scan. In contrast our images had smaller sized "tumors" (1 deg) added at random locations within the scans.

Moreover, adaptation increases early neural responses regardless of target presence or absence (Figure 29, panels a-b and c-d). Our present findings mirror a previous study demonstrating that adaptation to facial stimuli caused an enhancement in the neural response at the early P1 component (Kloth & Schweinberger, 2010). Previous research has shown an attenuation of the neural response following adaptation, suggesting that adaptation functions to decrease neuronal resources devoted to the unchanging scene thereby increasing the salience of infrequent stimuli and enhancing the magnitude of the response (Kloth & Schweinberger, 2010; Schweinberger et al., 2007). Contrary to these previous findings, our results reveal increased magnitude of the response following adaptation. One possibility is that this conflicting result was due to increased attentional allocation for locating potential targets following adaptation. Previous research has demonstrated that attending to stimulus features can significantly modulate the waveform (for review:(Coull, 1998). Specifically, attentional mechanisms increase the amplitude of early components such as the P100 and N100 which is indicative of recruiting greater neuronal resources. The P100 is thought to reduce noise, while the N100 acts to increase the response to the attended stimuli. Moreover, attention has been shown to increase the neural activity in later components such as the P300 (for review:(Coull, 1998). These findings may provide an explanation as to why our results are inconsistent with previous reports. In these studies, participants were not tasked with signaling target detection or absence. Thus, adaptation may function to suppress processing of the background image, while increasing the response to the target

or to resources devoted to correctly rejecting images without targets. Further support for this is reflected in the increase in the amplitude of the waveform following adaptation. Future investigations will be necessary to determine if this is the case for the results presented here.

Prolonged exposure to fatty images resulted in decreased reaction times when searching on the same image type (fatty). This was not the case when inspecting dense images for targets (Figure 32). This is in contrast to our previous findings showing increased search efficiency when searching on the same image type as adapt, for both dense and fatty images (Chapter IV). It could be that observers did not adapt to density, and thus detection of the "tumors" was not facilitated post adaptation. Indeed, observers reported after adapting to fatty images they felt as if targets were easier to detect but did not report that adaptation to dense images aided in locating the targets more efficiently. Additionally, the topographical analysis revealed increased activity for fatty trials following adaptation to fatty scans in comparison to dense (Figure 31 and 32). These results could suggest increased search efficiency when inspecting fatty scans for targets.

Taken together these results have implications regarding inspection in a radiological environment. For instance, radiologists report having diverse search routines, often reporting that they inspect and classify scans in an arbitrary order rather than by density type. Our results suggest that prior exposure to the image type (dense or fatty) one is inspecting for lesions or tumors could better facilitate detection. This could contribute to not only a reduction in the time devoted to

each scan, but consequently reduce fatigue. Moreover, this is the only known study to investigate the electrophysiological correlates of medical image adaptation. Importantly, these studies were conducted using untrained naïve observers and expertly trained radiologists may show different patterns of neuronal activation than untrained participants. This could provide further insight into how expertise modulates the magnitude of the waveforms as well as the influence of adaptation.

VI. General Discussion

The present research explored the role of adaptation and medical image perception. Little to no research has investigated how the process of visual adaptation may influence observers' visual sensitivity and perception of radiological scans. Moreover, radiologists are tasked with classifying and diagnosing medical images based upon subjective visual inspection. Critically, this evaluation process is ultimately constrained by the perceptual and cognitive capabilities of the observer (E. A. Krupinski, 2011). Due to the fact that radiologists can spend hours at a time inspecting mammogram images this process seems likely to lead to pronounced adaptation. Importantly, medical images are classified by their textural properties using the BI-RADS Density classification system on a scale from fatty to dense ((ACR), 1998). These classifications are important because they have been correlated with potential prevalence of cancer (Boyd et al., 2007). Ultimately radiologists are tasked with inspecting images for abnormalities and this task has important health

consequences. The goal of this dissertation was to investigate the influence of adaptation on the classification and inspection of mammogram images.

Summary of Findings

The goal of the first experiment (Chapter II) was to investigate how visual adaptation influences the appearance of medical images, particularly the textural properties that are used to classify them. Our results revealed that simply viewing the different textural properties used to categorize medical images strongly biased subsequent image classification. Moreover, prolonged exposure to dense (fatty) images not only resulted in the following images appearing more fatty (dense), but the adapting image itself appeared less dense over time. These findings are analogous to previous studies investigating adaptation to color and facial characteristics, which showed that exposure to these stimulus properties resulted in the adapting image appearing less distinct and more neutral over time (M. A. Webster & MacLeod, 2011). This supports a form of renormalization of coding to the textural properties of the mammogram images, possibly to highlight changes from the current stimulus dimension (dense or fatty) (Rhodes et al., 2005; M. A. Webster & MacLeod, 2011).

In experiment 2 (Chapter III), we investigated how adaptation to the unique statistical properties of the images would influence the perception of blur and contrast sensitivity. Specifically, radiological images have a steeper amplitude spectra than that of natural images, causing them to appear blurrier in appearance (Burgess et al., 2001; Field & Brady, 1997). Observers strongly

adapted to the characteristic properties of the radiological scans, resulting in the expected blur aftereffects. Viewing of the original mammogram images caused focused images to appear over-sharpened following adaptation. These results suggest that observers adapt not only to the textural properties of the scans, but also the characteristic statistical properties of the images.

These previous findings showed that participants strongly adapted to the properties of mammogram images and this affected the appearance of subsequent scans. Experiment 3 (Chapter IV) aimed at exploring if adaptation to the structure of the medical images would influence detection of simulated tumors within the scans. Adaptation to the different textural properties of the scans enhanced detection of novel targets within the images. Moreover, adaptation to a particular image type, dense or fatty, enhanced search upon the same image type. For example, if an individual was previously adapted to a fatty (dense) array of images, reaction time was reduced when searching on fatty (dense) images, but not dense (fatty). As discussed above, these results suggest adaptation may function to discount properties of the unchanging background scene in order to enhance detection of novel, uncharacteristic features within the image.

Our last study (Chapter V) explored where in the visual processing stream these visual aftereffects are manifesting. By utilizing ERP's while observers were adapting to the mammogram scans we were able to test for electrophysiological signatures involved in the classification and detection of targets within the images. Interestingly, adaptation produced non-significant differences in the

component waveforms when categorizing the images based upon their textural properties. However, when participants were instead tasked with signaling the presence or absence of a target, prolonged exposure to the medical images significantly affected the magnitude of the neural response. Specifically, adaptation increased the amplitude of the response in early and late occipital areas. This is consistent with previous studies demonstrating an increase in the P300 component when inspecting mammogram images for simulated tumors (Hope et al., 2013). Moreover, the coding of texture has been shown to occur in occipito-temporal cortex and thus, adaptation in these areas seems likely (Cant & Goodale, 2007; Cant et al., 2008). Unlike previous ERP studies adaptation did not attenuate the component waveforms response in earlier visual areas (Kloth & Schweinberger, 2010; Schweinberger et al., 2007). Our results suggest that adaptation may function to allocate greater attentional resources in order to perform the detection task. We hypothesize that by recruiting greater neuronal resources the observer is better able to detect abnormalities within the scan (for review:(Coull, 1998).

Implications and Future Directions

The primary goal of this dissertation was to provide a comprehensive analysis of the influence of adaptation on the visually important task of inspecting and diagnosing radiological images. Interestingly, radiologists use diverse techniques when inspecting and classifying medical images. Specifically, they report viewing the images in an arbitrary order based largely upon the order they

are received in. Our findings have implications regarding the influence of ordering effects on their current state of adaptation. Our results revealed strong and rapid adaptation to the textural properties of the mammograms, thus viewing them in an arbitrary order may influence subsequent categorization of the next scan. For example, if presently viewing a fatty scan and then switch to inspecting a dense scan, this could potentially bias their classification of the current image. Moreover, we showed that prolonged exposure to an image resulted in the adapting image appearing less distinct over time. This form of renormalization of coding dimension to the current stimulus under inspection has potential implications for optimizing visual inspection of the images.

Adaptation to a specific image type (dense or fatty) facilitated detection of targets when searching on the same image type as the adapt. Thus, adaptation may function to optimize performance by discounting the unchanging background characteristics of the scans and highlight novel features, or abnormalities within the scans. These results suggest that viewing mammogram images by density classification may not only facilitate correct categorization, but more importantly enhance detection of novel features within the images. Moreover, previous research has demonstrated that radiologists are able to rapidly and accurately diagnose images containing abnormalities (Drew et al., 2013; E.A . Krupinski, 1996; Kundel & Follette, 1972; Kundel & Nodine, 1975; Kundel et al., 2008; Mugglestone et al., 1995). This suggests radiologists are able to compare the current image under inspection to an internal template of what is normal or expected within the images, enabling the radiologist to direct their attention to

areas of interest (Kundel et al., 1987; Swensson, 1980). Our results suggest that adaptation may facilitate this process by enabling readers to more efficiently direct attention to areas containing abnormalities. Thus, as discussed above, viewing images based upon density type may enhance the inspection process by reducing the amount of time that needs to be devoted to each image, consequently reducing the amount of fatigue radiologists encounter during this process.

It is important to note that our studies used naïve, untrained participants. Thus future work has yet to explore how the effects of adaptation manifest in an actual medical environment. We aim to explore these studies with expertly trained radiologists. It is possible that radiologists have a different pattern of adaptation than untrained observers. For instance, radiologists may have the ability to switch into an adapted state quicker when inspecting mammogram images, similar to the way in which individuals are able to rapidly adjust to their visual correction. Moreover, it would be interesting to investigate the influence of adaptation while individuals are being trained to be radiologists. Much as search improves through training (Snowden et al., 2000), adaptation may functionally change as individuals become experts in the field. These are questions we hope to explore in the future, providing a better understanding of not only the role of adaptation in a medical environment, but also how expertise is influenced by adaptation.

References

(ACR), A. C. o. R. (1998). *Breast Imaging Reporting and Data System (BI-RADS)* (3rd ed.). Reston, VA: American College of Radiology.

Abbonizio, G., Langley, K., & Clifford, C. W. G. (2002). Contrast adaptation may enhance contrast discrimination. [Article]. *Spatial Vision, 16*(1), 45-58. doi: 10.1163/15685680260433904

Anokhin, A. P., Golosheykin, S., Sirevaag, E., Kristjansson, S., Rohrbaugh, J. W., & Heath, A. C. (2006). Rapid discrimination of visual scene content in the human brain. *Brain Research, 1093*(1), 167-177. doi: http://dx.doi.org/10.1016/j.brainres.2006.03.108

Antal, A., Kéri, S., Kovács, G., Janka, Z., & Benedek, G. (2000). Early and late components of visual categorization: an event-related potential study. *Cognitive Brain Research, 9*(1), 117-119. doi: http://dx.doi.org/10.1016/S0926-6410(99)00053-1

Antal, A., Kéri, S., Kovács, G., Liszli, P., Janka, Z., & Benedek, G. (2001). Event-related potentials from a visual categorization task. *Brain Research Protocols, 7*(2), 131-136. doi: http://dx.doi.org/10.1016/S1385-299X(01)00055-1

Bao, M., & Engel, S. A. (2012). Distinct mechanism for long-term contrast adaptation. *Proc Natl Acad Sci U S A, 109*(15), 5898-5903. doi: 1113503109 [pii]10.1073/pnas.1113503109

Belmore, S. C., & Shevell, S. K. (2010). Very-long-term and short-term chromatic adaptation: are their influences cumulative? *Vision Res, 51*(3), 362-366. doi: S0042-6989(10)00564-X [pii]10.1016/j.visres.2010.11.011

Bex, P. J., Solomon, S. G., & Dakin, S. C. (2009). Contrast sensitivity in natural scenes depends on edge as well as spatial frequency structure. *J Vis, 9*(10), 1 1-19. doi: 10.1167/9.10.1/9/10/1/ [pii]

Bochud, F., Abbey, C., & Eckstein, M. (1999). Statistical texture synthesis of mammographic images with super-blob lumpy backgrounds. *Opt Express, 4*(1), 33-42.

Boyd, N. F. (2011). Tamoxifen, mammographic density, and breast cancer prevention. [CommentEditorial]. *J Natl Cancer Inst, 103*(9), 704-705. doi: 10.1093/jnci/djr115

Boyd, N. F., Guo, H., Martin, L. J., Sun, L., Stone, J., Fishell, E., . . . Yaffe, M. J. (2007). Mammographic density and the risk and detection of breast cancer. [Research Support, Non-U.S. Gov't]. *N Engl J Med, 356*(3), 227-236. doi: 10.1056/NEJMoa062790

Brainard, D. H. (1997). The Psychophysics Toolbox. *Spat Vis, 10*(4), 433-436.

Burgess, A. E., Jacobson, F. L., & Judy, P. F. (2001). Human observer detection experiments with mammograms and power-law noise. [Research Support, U.S. Gov't, P.H.S.]. *Med Phys, 28*(4), 419-437.

Burgess, A. E., Li, X., & Abbey, C. K. (1997). Visual signal detectability with two noise components: anomalous masking effects. [Comparative Study Research Support, U.S. Gov't, P.H.S.]. *J Opt Soc Am A Opt Image Sci Vis, 14*(9), 2420-2442.

Cant, J. S., Arnott, S. R., & Goodale, M. A. (2009). fMR-adaptation reveals separate processing regions for the perception of form and texture in the human ventral stream. *Experimental Brain Research, 192*(3), 391-405. doi: 10.1007/s00221-008-1573-8

Cant, J. S., & Goodale, M. A. (2007). Attention to Form or Surface Properties Modulates Different Regions of Human Occipitotemporal Cortex. *Cerebral Cortex, 17*(3), 713-731. doi: 10.1093/cercor/bhk022

Cant, J. S., Large, M. E., McCail, L., & Goodale, M. A. (2008). Independent processing of form, colour, and texture in object perception. *Perception, 37*(1), 57-78.

Chen, L., Abbey, C. K., Nosratieh, A., Lindfors, K. K., & Boone, J. M. (2012). Anatomical complexity in breast parenchyma and its implications for optimal breast imaging strategies. *Medical Physics, 39*, 7. doi: 10.1118/1.3685462

Clifford, C. W., Webster, M. A., Stanley, G. B., Stocker, A. A., Kohn, A., Sharpee, T. O., & Schwartz, O. (2007). Visual adaptation: neural, psychological and computational aspects. *Vision Research, 47*(25), 3125-3131. doi: S0042-6989(07)00375-6 [pii]10.1016/j.visres.2007.08.023

Clifford, C. W. G., Wyatt, A. M., Arnold, D. H., Smith, S. T., & Wenderoth, P. (2001). Orthogonal adaptation improves orientation discrimination. *Vision Research, 41*(2), 151-159. doi: http://dx.doi.org/10.1016/S0042-6989(00)00248-0

Coull, J. T. (1998). Neural correlates of attention and arousal: insights from electrophysiology, functional neuroimaging and psychopharmacology. *Progress in Neurobiology, 55*(4), 343-361. doi: http://dx.doi.org/10.1016/S0301-0082(98)00011-2

De Valois, R. L., & De Valois, K. K. (1990). Spatial Vision. *New York: Oxford University Press*.

Delahunt, P. B., Webster, M. A., Ma, L., & Werner, J. S. (2004). Long-term renormalization of chromatic mechanisms following cataract surgery. *Visual Neuroscience, 21*(3), 301-307.

Delorme, A., Rousselet, G. A., Macé, M. J. M., & Fabre-Thorpe, M. (2004). Interaction of top-down and bottom-up processing in the fast visual analysis of natural scenes. *Cognitive Brain Research, 19*(2), 103-113. doi: http://dx.doi.org/10.1016/j.cogbrainres.2003.11.010

Donovan, T., & Litchfield, D. (2013). Looking for Cancer: Expertise Related Differences in Searching and Decision Making. *Applied Cognitive Psychology, 27*(1), 43-49. doi: 10.1002/acp.2869

Drew, T., Evans, K., Vo, M. L., Jacobson, F. L., & Wolfe, J. M. (2013). Informatics in radiology: what can you see in a single glance and how might this guide visual search in medical images? [Research Support, N.I.H., Extramural]. *Radiographics, 33*(1), 263-274. doi: 10.1148/rg.331125023

Durgin, F. H. (2008). Texture density adaptation and visual number revisited. *Curr Biol, 18*(18), R855-856; author reply R857-858. doi: S0960-9822(08)00962-7 [pii]10.1016/j.cub.2008.07.053

Durgin, F. H., & Huk, A. C. (1997). Texture Density Aftereffects in the Perception of Artificial and Natural Textures. *Vision Research, 37*, 3273-3282.

Durgin, F. H., & Proffitt, D. R. (1996). Visual learning in the perception of texture: simple and contingent aftereffects of texture density. *Spat Vis, 9*(4), 423-474.

Eckstein, M. P. (2011). Visual search: a retrospective. [Research Support, N.I.H., ExtramuralResearch Support, Non-U.S. Gov'tResearch Support, U.S. Gov't, Non-P.H.S.Review]. *J Vis, 11*(5). doi: 10.1167/11.5.14

Eckstein, M. P., Abbey, C. K., & Bochud, F. O. (2000). A practical guide to model observers for visual detection in synthetic and natural noisy images Handbook of Medical Imaging *Handbook of Medical Imaging, 1*, 593-628.

Elliott, S. L., Georgeson, M. A., & Webster, M. A. (2011). Response normalization and blur adaptation: Data and multi-scale model. *J Vis, 11*(2). doi: 11.2.7 [pii]10.1167/11.2.7

Evans, K. K., Birdwell, R. L., & Wolfe, J. M. (2013). If you don't find it often, you often don't find it: why some cancers are missed in breast cancer screening. *PLoS One, 8*(5), e64366. doi: 10.1371/journal.pone.0064366

Field, D. J. (1987). Relations between the statistics of natural images and the response properties of cortical cells. *Journal of the Optical Society of America A, 4*(12), 2379-2394. doi: 10.1364/josaa.4.002379

Field, D. J., & Brady, N. (1997). Visual sensitivity, blur and the sources of variability in the amplitude spectra of natural scenes. *Vision Research, 37*(23), 3367-3383. doi: http://dx.doi.org/10.1016/S0042-6989(97)00181-8

Gale, A. (19884). Medical image perception. *Elsevier Sci Pub*, 295.

Greene, M. R., & Oliva, A. (2010). High-level aftereffects to global scene properties. *J Exp Psychol Hum Percept Perform, 36*(6), 1430-1442. doi: 2010-17520-001 [pii]10.1037/a0019058

Gur, D., Sumkin, J. H., Rockette, H. E., Ganott, M., Hakim, C., Hardesty, L., . . . Wallace, L. (2004). Changes in Breast Cancer Detection and Mammography Recall Rates After the Introduction of a Computer-Aided Detection System. *J Natl Cancer Inst, 96*(3), 185-190. doi: 10.1093/jnci/djh067

Harris, H., Gliksberg, M., & Sagi, D. (2012). Generalized perceptual learning in the absence of sensory adaptation. [Research Support, Non-U.S. Gov't]. *Curr Biol, 22*(19), 1813-1817. doi: 10.1016/j.cub.2012.07.059

Hersh, M., & Marla, R. (2004). Imaging the dense breast. *Applied Radiology, 33*, 23-27.

Hope, C., Sterr, A., Elangovan, P., Geades, N., Young, K., & Wells, K. (2013). High throughput screening for mammography using a human-computer interface with rapid serial visual presentation (RSVP). *Proc. SPIE* doi: doi:10.1117/12.2007557

Horowitz, T. S., Kenner, N. M., & Wolfe, J. M. (2005). Rare items often missed in visual searches. *Nature.*

Johnson, J. S., & Olshausen, B. A. (2003). Timecourse of neural signatures of object recognition. *J Vis, 3*(7). doi: 10.1167/3.7.4

Johnson, J. S., & Olshausen, B. A. (2005). The earliest EEG signatures of object recognition in a cued-target task are postsensory. *J Vis, 5*(4). doi: 10.1167/5.4.2

Kirchner, H., & Thorpe, S. J. (2006). Ultra-rapid object detection with saccadic eye movements: Visual processing speed revisited. *Vision Research, 46*(11), 1762-1776. doi: http://dx.doi.org/10.1016/j.visres.2005.10.002

Kloth, N., & Schweinberger, S. R. (2010). Electrophysiological correlates of eye gaze adaptation. *J Vis, 10*(12). doi: 10.1167/10.12.17

Kohn, A. (2007). Visual adaptation: physiology, mechanisms, and functional benefits. *J Neurophysiol, 97*(5), 3155-3164. doi: 00086.2007 [pii] 10.1152/jn.00086.2007

Kompaniez, E., Abbey, C. K., Boone, J. M., & Webster, M. A. (2013). Adaptation aftereffects in the perception of radiological images. *PLoS One, in press*. doi: 10.1371/journal.pone.0076175

Kompaniez, E., Sawides, L., Marcos, S., & Webster, M. A. (2013). Adaptation to interocular differences in blur. *J Vis, 13*(6). doi: 10.1167/13.6.19

Kording, K. P., Tenenbaum, J. B., & Shadmehr, R. (2007). The dynamics of memory as a consequence of optimal adaptation to a changing body. *Nat Neurosci, 10*(6), 779-786. doi: nn1901 [pii]10.1038/nn1901

Kovács, G., Zimmer, M., Bankó, É., Harza, I., Antal, A., & Vidnyánszky, Z. (2006). Electrophysiological Correlates of Visual Adaptation to Faces and Body Parts in Humans. *Cerebral Cortex, 16*(5), 742-753. doi: 10.1093/cercor/bhj020

Kristjánsson, Á. (2011). The Functional Benefits of Tilt Adaptation. [Article]. *Seeing & Perceiving, 24*(1), 37-51. doi: 10.1163/187847511x555283

Krupinski, E. A. (1996). Visual scanning patterns of radiologists searching mammograms. *ACADEMIC RADIOLOGY*.

Krupinski, E. A. (2011). The role of perception in imaging: past and future. *Semin Nucl Med, 41*(6), 392-400. doi: 10.1053/j.semnuclmed.2011.05.002

Kundel, H. L. (2004). Reader error, object recognition and visual search. *Image Perception, Observer Performance, and Technology Assessment, 1*. doi: doi:10.1117/12.542717

Kundel, H. L., & Follette, P. S. (1972). Visual search patterns and experience with radiological images. *Radiology*.

Kundel, H. L., & Nodine, C. F. (1975). Interpreting chest radiographs without visual search. *Radiology*.

Kundel, H. L., Nodine, C. F., Krupinski, E. A., & Mello-Thomas, C. (2008). Using gaze-tracking data and mixture distribution analysis to support a holistic model for the detection of cancers on mammograms. *ACADEMIC RADIOLOGY, 15*(881 - 886). doi: 10.1016/j.acra.2008.01.023

Kundel, H. L., Nodine, C. F., Thickman, D., & Toto, L. (1987). Searching for lung nodules a comparison of human performance with random and systematic scanning. *investigative radiology*.

Kwon, M., Legge, G. E., Fang, F., Cheong, A. M., & He, S. (2009). Adaptive changes in visual cortex following prolonged contrast reduction. *J Vis, 9*(2), 20 21-16. doi: 10.1167/9.2.20/9/2/20/ [pii]

Liu, H., Agam, Y., Madsen, J. R., & Kreiman, G. (2009). Timing, Timing, Timing: Fast Decoding of Object Information from Intracranial Field Potentials in Human

Visual Cortex. *Neuron, 62*(2), 281-290. doi:http://dx.doi.org/10.1016/j.neuron.2009.02.025

Mace, M. J. M., Joubert, O. R., Nespoulous, J. L., & Fabre-Thorpe, M. (2009). The time-course of visual categorization: you spot than animal faster than the bird. *PLoS One*. doi: http://dx.doi.org/10.1371%2Fjournal.pone.0005927

Manning, D. J., Gale, A., & Krupinski, E. A. (2005). Perception research in medical imaging. *Br J Radiol, 78*(932), 683-685. doi: 10.1259/bjr/72087985

McDermott, K. C., Malkoc, G., Mulligan, J. B., & Webster, M. A. (2010). Adaptation and visual salience. *J Vis, 10*(13), 17. doi: 10.13.17 [pii]10.1167/10.13.17

Motoyoshi, I., Nishida, S., Sharan, L., & Adelson, E. H. (2007). Image statistics and the perception of surface qualities. *Nature, 447*(7141), 206-209. doi: nature05724 [pii]10.1038/nature05724

Mugglestone, M. D., Gale, A. G., Cowley, H. C., & Wilson, A. R. M. (1995). Diagnostic performance on briefly presented mammographic images. *SPIE*.

Neitz, J., Carroll, J., Yamauchi, Y., Neitz, M., & Williams, D. R. (2002). Color perception is mediated by a plastic neural mechanism that is adjustable in adults. *Neuron, 35*(4), 783-792. doi: S0896627302008188 [pii]

Niedeggen, M., & Wist, E. R. (1998). The physiological substrate of motion afetreffects. *In: The Motion Aftereffect: A Modern Perspective, MA: MIT Press*, 125-155.

Ouhnana, M., Bell, J., Morgan. M.J., Solomon, J. A., & Kingdom, F. A. A. (2013). After-effect of perceived regularity. *Journal of Vision, 11*. doi: 10.1167/11.11.1084

Paller, K., McCarthy, G., Roessler, E., Allison, T., & Wood, C. (1992). POTENTIALS-EVOKED IN HUMAN AND MONKEY MEDIAL TEMPORAL-LOBE DURING AUDITORY AND VISUAL ODDBALL PARADIGMS. *ELECTROENCEPHALOGRAPHY AND CLINICAL NEUROPHYSIOLOGY, 84*.

Picton, T. (1992). The P300 of the event-related potential. *Journal of Clinical Neurophysiology*, 456 – 479.

Piotrowski, L. N., & Campbell, F. W. (1982). A demonstration of the visual importance and flexibility of spatial-frequency amplitude and phase. *Perception, 11*(3), 337-346.

Polich, J., & Kok, A. (1995). Cognitive and biological determinants of P300: an integrative review. *Biological Psychology, 41*(2), 103-146. doi: http://dx.doi.org/10.1016/0301-0511(95)05130-9

Rhodes, G., Robbins, R., Jaquet, E., McKone, E., Jeffery, L., & Clifford, C. W. G. (2005). Adaptation and face perception - how aftereffects implicate norm based coding of faces. In C. W. G. Clifford & G. Rhodes (Eds.), *Fitting the Mind to the World: Adaptation and Aftereffects in High-Level Vision* (pp. 213-240). Oxford: Oxford University Press.

Rousselet, G. A., Macé, M. J. M., Thorpe, S. J., & Fabre-Thorpe, M. (2007). Limits of Event-related Potential Differences in Tracking Object Processing Speed. *Journal of Cognitive Neuroscience, 19*(8), 1241-1258. doi: 10.1162/jocn.2007.19.8.1241

Rugg, M. D., Doyle, M. C., & Wells, T. (1995). Word and Nonword Repetition Within- and Across-Modality: An Event-Related Potential Study. *Journal of Cognitive Neuroscience, 7*(2), 209-227. doi: 10.1162/jocn.1995.7.2.209

Sawides, L., de Gracia, P., Dorronsoro, C., Webster, M., & Marcos, S. (2011). Adapting to blur produced by ocular high-order aberrations. *J Vis, 11*(7). doi: 10.1167/11.7.21

Sawides, L., Marcos, S., Ravikumar, S., Thibos, L., Bradley, A., & Webster, M. (2010). Adaptation to astigmatic blur. *J Vis, 10*(12), 22. doi: 10.12.22 [pii] 10.1167/10.12.22

Schweinberger, S. R., Kloth, N., & Jenkins, R. (2007). Are you looking at me? Neural correlates of gaze adaptation. *Neuroreport, 18*(7), 693-696.

Sharpee, T. O., Sugihara, H., Kurgansky, A. V., Rebrik, S. P., Stryker, M. P., & Miller, K. D. (2006). Adaptive filtering enhances information transmission in visual cortex. [10.1038/nature04519]. *Nature, 439*(7079), 936-942. doi: http://www.nature.com/nature/journal/v439/n7079/suppinfo/nature04519_S1.html

Simoncelli, E. P., & Olshausen, B. A. (2001). NATURAL IMAGE STATISTICS AND NEURAL REPRESENTATION. *Annual Review of Neuroscience, 24*(1), 1193-1216. doi: doi:10.1146/annurev.neuro.24.1.1193

Snowden, P. T., Davies, I. R. L., & Roling, P. (2000). Perceptual learning of the detection of features in X-ray images: A functional role for improvements in adults' visual sensitivity? *Journal of Experimental Psychology: Human perception and performance, 26*(1), 379-390. doi: 10.1037/0096-1523.26.1.379

Swensson, R. G. (1980). A two-stage detection model applied to skilled visual search by radiologists. *Perception & Psychophysics.*

Tadmor, Y., & Tolhurst, D. J. (1993). Both the phase and the amplitude spectrum may determine the appearance of natural images. *Vision Res, 33*(1), 141-145.

Thompson, P., & Burr, D. (2009). Visual aftereffects. *Curr Biol, 19*(1), R11-14. doi: S0960-9822(08)01346-8 [pii]10.1016/j.cub.2008.10.014

Thorpe, S., Fize, D., & Marlot, C. (1996). Speed of processing in the human visual system. [10.1038/381520a0]. *Nature, 381*(6582), 520-522.

Tolhurst, D., Tadmor, Y., & Chao, T. (1992). Amplitude spectra of natural images. *OPHTHALMIC AND PHYSIOLOGICAL OPTICS, 12*.

VanRullen, R., & Thorpe, S. J. (2001). The Time Course of Visual Processing: From Early Perception to Decision-Making. *Journal of Cognitive Neuroscience, 13*(4), 454-461. doi: 10.1162/08989290152001880

Vera-Diaz, F. A., Woods, R. L., & Peli, E. (2010). Shape and individual variability of the blur adaptation curve. *Vision Res, 50*(15), 1452-1461. doi: S0042-6989(10)00187-2 [pii]10.1016/j.visres.2010.04.013

Vul, E., Krizay, E., & MacLeod, D. I. (2008). The McCollough effect reflects permanent and transient adaptation in early visual cortex. *J Vis, 8*(12), 4 1-12. doi: 10.1167/8.12.4/8/12/4/ [pii]

Watson, A. B., & Ahumada, A. J. (2011). Blur clarified: A review and synthesis of blur discrimination. *J Vis, 11*(5). doi: 10.1167/11.5.10

Webster, M., Mizokami, Y., Svec, L., & Elliott, S. (2006). Neural adjustments to chromatic blur. *Spatial Vision, 19*(2), 111-132. doi:10.1163/156856806776923380

Webster, M. A. (2011a). Adaptation and visual coding. *J Vis, 11*(5), 3: 1-23. doi: 11.5.3 [pii]10.1167/11.5.3

Webster, M. A. (2011b). Adaptation and visual coding. *Journal of Vision*. doi: 10.1167/11.5.3

Webster, M. A., Georgeson, M. A., & Webster, S. M. (2002). Neural adjustments to image blur. *Nature Neuroscience, 5*(9), 839-840. doi: 10.1038/nn906nn906

Webster, M. A., & Juricevic, I. (2013). Optimizing visual performance by adapting images to observers. *SPIE, 8651-21*.

Webster, M. A., & Leonard, D. (2008). Adaptation and perceptual norms in color vision. *Journal of the Optical Society of America A, 25*(11), 2817-2825. doi: 172996 [pii]

Webster, M. A., & MacLeod, D. I. A. (2011). Visual adaptation and face perception. *Philos Trans R Soc Lond B Biol Sci, 366*(1571), 1702-1725. doi: 366/1571/1702 [pii] 10.1098/rstb.2010.0360

Webster, M. A., & Miyahara, E. (1997). Contrast adaptation and the spatial structure of natural images. *J Opt Soc Am A Opt Image Sci Vis, 14*(9), 2355-2366.

Wissig, S. C., Patterson, C. A., & Kohn, A. (2013). Adaptation improves performance on a visual search task. [Research Support, N.I.H., Extramural Research Support, Non-U.S. Gov't Research Support, U.S. Gov't, Non-P.H.S.]. *J Vis, 13*(2), 6. doi: 10.1167/13.2.6

Wolfe, J. M., Horowitz, T. S., Van Wert, M. J., Kenner, N. M., Place, S. S., & Kibbi, N. (2007). Low target prevalence is a stubborn source of errors in visual search tasks. *Journal of Experimental Psychology: General, 136*(4), 623-638. doi: 10.1037/0096-3445.136.4.623

Yehezkel, O., Sagi, D., Sterkin, A., Belkin, M., & Polat, U. (2010). Learning to adapt: Dynamics of readaptation to geometrical distortions. *Vision Res, 50*(16), 1550-1558. doi: S0042-6989(10)00235-X [pii] 10.1016/j.visres.2010.05.014